Supporting Information

Formic Acid Catalyzed Isomerization and Adduct Formation of an Isoprene-Derived Criegee Intermediate: Experiment and Theory

Michael F. Vansco[1], Rebecca L. Caravan[2,3,4*], Shubhrangshu Pandit[1,5], Kristen Zuraski[2], Frank A. F. Winiberg[6,7], Kendrew Au[3], Trisha Bhagde[1], Nisalak Trongsiriwat[1], Patrick J. Walsh[1], David L. Osborn[3], Carl J. Percival[6], Stephen J. Klippenstein[4], Craig A. Taatjes[3], and Marsha I. Lester[1**]

[1]Department of Chemistry, University of Pennsylvania, Philadelphia, PA 19104-6323, USA.
[2]NASA Postdoctoral Program Fellow, NASA Jet Propulsion Laboratory, California Institute of Technology, 4800 Oak Grove Drive, Pasadena, CA 91109, USA.
[3]Combustion Research Facility, Mailstop 9055, Sandia National Laboratories, Livermore, CA 94551, USA.
[4]Chemical Sciences and Engineering Division, Argonne National Laboratory, Lemont, IL 60439, USA.
[5]Department of Chemistry and Biochemistry, University of California San Diego, La Jolla, CA 92093, USA
[6]NASA Jet Propulsion Laboratory, California Institute of Technology, 4800 Oak Grove Drive, Pasadena, CA 91109, USA.
[7]Division of Chemistry and Chemical Engineering, California Institute of Technology, Pasadena, CA 91125, USA.

[*] Corresponding author email: caravarl@anl.gov
[**]Corresponding author email: milester@sas.upenn.edu

Table of Contents:

Section S1. MVK-oxide + H_2-formic acid

The identification of HPBD at m/z 87 in the D_2-formic acid experiments (discussed in the main text) is also supported by the time profiles of the m/z 86 data obtained in experiments using normal H_2-formic acid. With increasing formic acid concentration, an increase in signal appearing as a y-axis offset is observed at longer kinetic times in the time profiles of m/z 86 (Figure S1, *bottom*). The increase in absolute signal of m/z 86 at longer kinetic times (Figure S1, *top*) is indicative of increased production of an isomer of MVK-oxide that can be photoionized at 10.5 eV and is stable on the timescale and conditions of our experimental conditions (10 Torr, 298 K), such as HPBD from the acid catalyzed isomerization mechanism. The relative photoionization cross-sections of Criegee intermediates and their respective vinyl hydroperoxide isomers calculated by Huang *et al.*[1] indicates that the cross-sections of the latter are significantly larger than the former. The magnitude of the y-axis offset in the m/z 86 time profiles with respect to the $t = 0$ signal amplitude (Figure S1, *bottom*) is, therefore consistent with the small yield of HPBD determined from the D_2-formic acid experiments and calculated through high-level theoretical kinetics, as discussed in the main text.

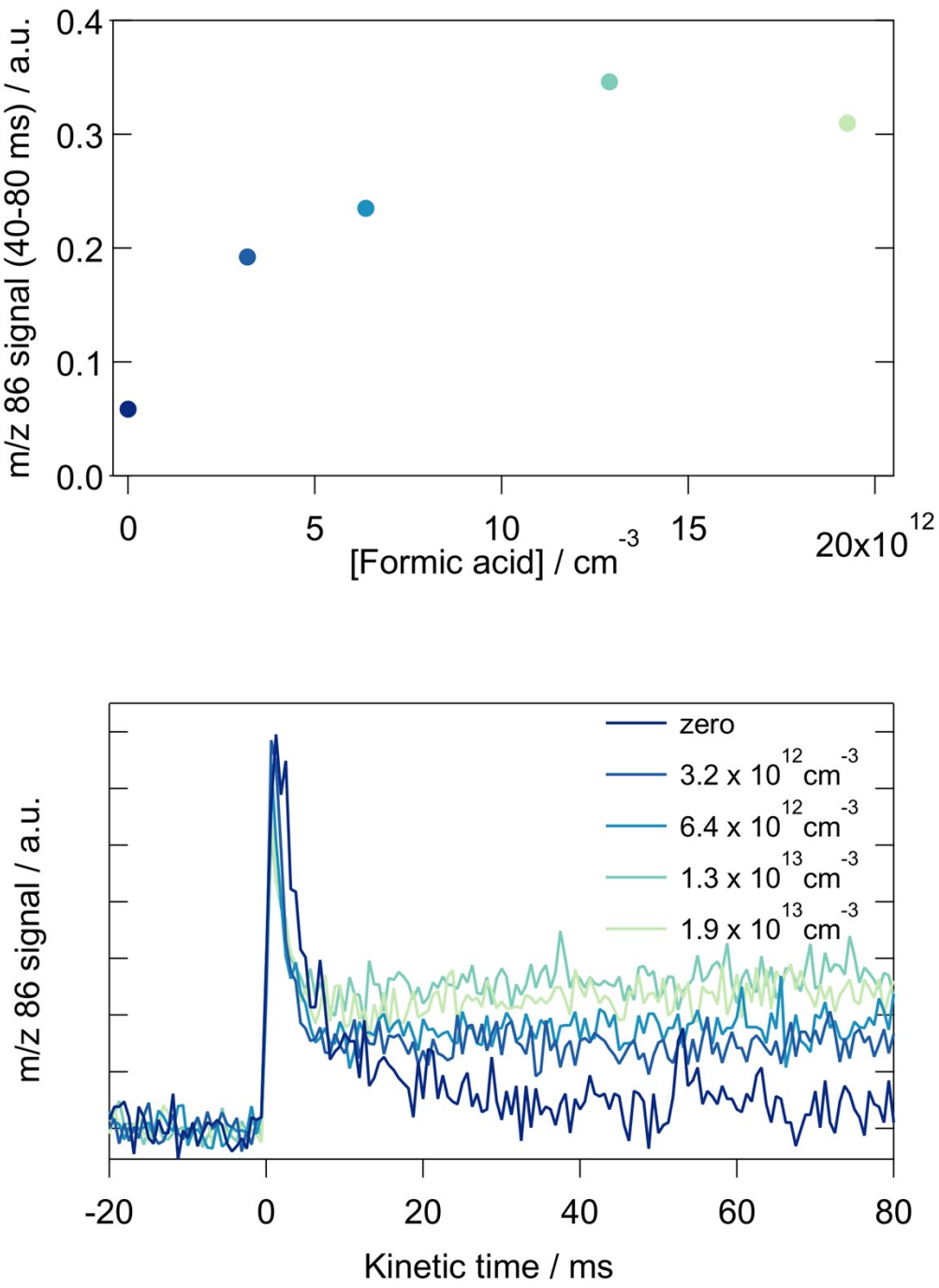

Figure S1. *Top* Summed absolute amplitudes of the m/z 86 signal (between 40-80 ms) in the MVK-oxide + H_2-formic acid reaction as a function of formic acid concentration, obtained using a photoionization energy of 10.5 eV. *Bottom* Time profiles of the m/z 86 signal, presented in the top figure, recorded at various formic acid concentrations. The data are each normalized for their experimental conditions (e.g. MVK-oxide precursor concentration, photolysis laser power and the photocurrent of the 10.5 eV photoionization radiation) using the maxima in the amplitudes of the respective I atom time traces as a reference.

Section S2: Theoretical reaction pathways

Overview

The present theoretical effort provides a detailed analysis of the kinetics for the reaction of MVK-oxide with formic acid (FA). It builds from the theoretical analysis presented in our prior study for the reaction of *syn-trans* MVK-oxide with FA,[2] with explorations of a variety of additional channels, and with an exploration of the kinetics for all four conformers of MVK-oxide. The primary focus is on the inclusion of the chemical catalysis channel that is observed experimentally in the present study, and which was previously explored theoretically in the work of Kumar et al. at the CCSD(T)/aug-cc-pVTZ//M06-2X/cc-pVTZ level.[3] The present analysis expands on that earlier theoretical work with more definitive ab initio electronic structure calculations, exploration of additional reaction channels, and, most significantly, through the implementation of *a priori* kinetic estimates. For completeness, we explore (i) analogues of the low-lying transition states explored by Vereecken and coworkers in their study of the reaction of CH_2OO with FA,[4] (ii) spectator catalysis, (iii) *cis-trans* isomerization in reactant pre-reactive complexes (PRCs), (iv) new reaction channels for the *anti* conformers, and (v) isotope exchange in the product PRC. The *cis-trans* isomerizations in the PRCs dramatically modulate the product distributions for the *cis* reactants. The predicted isotope exchange rate for the reaction between hydroperoxyl butadiene (HPBD) and deuterated FA (D_2-formic acid) is used to delineate the possible role of isotopic exchange from HPBD (possibly formed as a secondary product in the photolytic generation of MVK-oxide) interfering with the isotopic observations of deuterated HPBD.

Stationary Point Energies

The stationary point energies for the various reaction channels in the reaction of all four conformers of MVK-oxide with FA were determined at the CCSD(T)-F12/cc-pVTZ-F12//B2PLYP-D3/cc-pVTZ level coupled with the following ad hoc correction. The CCSD(T) method is known to underestimate the stability of Criegee intermediates (CIs) due to significant multireference effects arising from resonances between zwitterionic and singlet diradical electronic configurations. Furthermore, these

multireference effects persist to some extent for both the entrance channel van der Waals wells (where the CI retains much of its chemical character) and the transition states connecting them chemically to product species [e.g., HPBD, HPBF (hydroperoxybut-3-en-2-yl formate) adduct, HPBD-2, and dioxole]. Calculations at the CCSDT(Q) level largely capture these multireference effects, but such CCSDT(Q) calculations are impractical for a system with 9 heavy atoms (5 C atoms and 4 O atoms). Our prior studies provide CCSDT(Q) corrections for both MVK-oxide isomerizations[5] and the chemical reaction of CH_2OO with SO_2.[2] Here we use those values to crudely estimate these corrections for the present system. In particular, the MVK-oxide PRCs and the *cis-trans* transition states within these PRCs are estimated to be raised relative to the reactants by 0.4 kcal mol^{-1}, the transition states for the chemical conversions from the PRCs are estimated to be raised relative to reactants by 0.8 kcal mol^{-1} and the products are estimated to be raised by 1.5 kcal mol^{-1}. We estimate the uncertainties in these corrections to be about 0.2 kcal mol^{-1} for the first two values, and about 0.4 kcal mol^{-1} for the last one.

The results of these calculations are reported in Table S1. Note that the present energies differ slightly from those reported in our earlier study of the *syn-trans* MVK-oxide + FA reaction.[2] This difference arises from the prior neglect of the above described ad hoc CCSDT(Q) correction due to our focus there on just the addition rate. Overall, we expect 2σ uncertainties in our predicted energies of about 0.6 kcal mol^{-1}. Zero-point energy (ZPE) corrections evaluated for the stationary points corresponding to the reaction of deuterated FA with *syn-trans* and *syn-cis* MVK-oxide are also reported in Table S1. Note that for the radical-radical PRCs [e.g., OBD…OH, where OBD is oxybutadiene – $CH_2CHC(O)CH_2$] we evaluate the energy of the triplet state complex in order to avoid multireference issues for singlet radical-radical pre-reactive complexes. It is our experience that typically the energies of singlet and triplet PRCs agree to within a few tenths of a kcal mol^{-1}. When necessary, we have employed random sampling of initial torsional angles to obtain the lowest conformers.

Table S2 presents stationary point energies (kcal mol^{-1}) for the FA catalyzed isomerization of *syn-trans*-MVK-oxide evaluated by two different methods, and compared with earlier calculations by Kumar et al.[3] We repeated the prior calculations of Kumar et al. since the differences between the present

Table S1. Stationary point energies (kcal mol^{-1}) for the reaction of *syn/anti-cis/trans* (*s/a-c/t*) MVK-oxide with formic acid (FA).[a] Energies include ZPE corrections and are reported relative to *s-t*-MVK-oxide.

Stationary Point	ωB97XD 6-31+G*	B2PLYPD3 cc-pVTZ	CCSD(T)-F12 cc-pVTZ-F12	E0[b]	Total[c]	Corr. Total[d]
			Reactants			
s-t-MVK-oxide + FA	0	0	0	0	0	0
s-c-MVK-oxide + FA	1.3	2.3	1.9	-0.2	1.8	1.8
a-t-MVK-oxide + FA	2.2	3.0	2.7	-0.1	2.6	2.6
a-c-MVK-oxide + FA	1.8	2.8	2.8	0.0	2.8	2.8
s-t-MVK-oxide + FA excited	5.1	4.5	4.2	-0.2	4.0	4.0
			van der Waals			
			Reactant Wells			
s-t-MVK-oxide…FA	-17.4	-17.0	-15.8	1.1 (1.1)	-14.7	-14.3
s-c-MVK-oxide…FA	-16.3	-15.1	-14.1	0.8 (0.8)	-13.2	-12.8
a-t-MVK-oxide…FA	-16.5	-15.9	-14.7	0.9	-13.8	-13.4
a-c-MVK-oxide…FA	-15.5	-14.8	-13.2	1.0	-12.1	-11.7
			Product Wells			
s-t-HPBD…FA	-20.8	-24.5	-24.3	1.5	-22.7	-21.2
s-c-HPBD…FA	-22.2	-26.5	-26.1	1.7	-24.4	-22.9
a-t-HPBD…FA	-18.8	-22.3	-22.2	1.4	-20.8	-19.3
a-c-HPBD…FA	-17.6	-21.5	-21.6	1.4	-20.3	-18.8
HPBD-2…FA	-7.8	-11.0	-10.1	0.9	-9.3	-7.8
Dioxole…FA	-37.6	-35.4	-36.3	2.6	-33.6	-32.1
^{3}OBD… FA…OH	-4.3	-5.2	-2.7	-1.8	-4.5	-3.0
			Transition States			
			cis/trans			
s-t-MVK-oxide = *s-c*-MVK-oxide	7.6	9.4	8.2	-0.6	7.5	7.9
a-t-MVK-oxide = *a-c*-MVK-oxide	11.1	13.0	11.6	-0.7	10.9	11.3
s-t-MVK-oxide…FA = *s-c*-MVK-oxide…FA	-11.9	-10.6	-10.2	0.4 (0.5)	-9.7	-9.3
a-t-MVK-oxide…FA = *a-c*-MVK-oxide…FA	-9.5	-8.4	-10.2	0.3	-9.9	-9.5
			H Transfer (TS1)			
s-t-MVK-oxide = *s-t*-HPBD	21.9	18.9	19.7	-2.5	17.2	18.0
s-c-MVK-oxide = *s-c*-HPBD	23.0	20.2	21.0	-2.6	18.4	19.2
			Acid Catalyzed – Spectator (TS_{spec})			
s-t-MVK-oxide…FA = *s-t*-HPBD…FA	9.3	5.8	8.1	-1.4	6.7	7.5
s-c-MVK-oxide…FA = *s-c*-HPBD…FA	10.3	6.8	9.2	-1.5	7.7	8.5
			Acid Catalyzed – Chemically (TS2)			
s-t-MVK-oxide…FA = *s-t*-HPBD…FA	-5.3	-6.7	-3.1	-1.8 (-1.4)	-4.9	-4.1
s-c-MVK-oxide…FA = *s-c*-HPBD…FA	-5.3	-6.2	-2.7	-1.9 (-1.4)	-4.6	-3.8
a-t-MVK-oxide…FA = *a-t*-HPBD…FA	-0.5	-0.8	1.9	-1.0	0.8	1.6
a-c- MVK-oxide…FA = *a-c*-HPBD…FA	2.5	2.0	4.7	-1.0	3.7	4.5

1,4 Insertion (TS3)						
s-t-MVK-oxide…FA = *s-t*-HPBF Adduct	-13.8	-14.5	-12.6	-0.9 (-0.1)	-13.5	-12.7
s-c-MVK-oxide…FA = *s-c*-HPBF Adduct	-13.2	-13.6	-11.9	-0.6 (-0.0)	-12.6	-11.8
a-t-MVK-oxide…FA = *a-t*-HPBF Adduct	-14.0	-14.7	-12.7	-1.0	-13.6	-12.8
a-c-MVK-oxide…FA = *a-c*-HPBF Adduct	-12.5	-13.2	-11.0	-0.8	-11.8	-11.0
1,2 Insertion ($TS_{1,2\text{-insertion}}$)						
s-t-MVK-oxide…FA = *s-t*-HPBF Adduct	-2.3	-1.4	0.4	0.4	0.6	1.4
Cyclic Addition – SOZ Formation (TS_{SOZ})						
s-t-MVK-oxide…FA = SOZ	3.9	3.9	3.7	1.7	5.4	6.2
s-t-MVK-oxide…FA = SOZ Geometry 2	3.7	3.9	3.7	1.7	5.5	6.3
Acid Catalysis at C_2H_3 (TS_{vinyl})						
a-t-MVK-oxide…FA = HPBD-2	6.2	4.3	8.3	-2.6	5.7	6.5
HPBD Product Acid Cataylsis ($TS_{H,exchange}$)						
s-t-HPBD…FA = *s-t*-HPBD…FA	-1.8	-9.1	-7.4	-2.1	-9.5	-8.0
s-c-HPBD…FA = *s-c*-HPBD…FA	-3.4	-11.2	-9.4	-1.9	-11.3	-9.8
a-t-HPBD…FA = *a-t*-HPBD…FA	-0.7	-8.0	-6.2	-2.3	-8.5	-7.0
a-c-HPBD…FA = *a-c*-HPBD…FA	-0.9	-8.6	-6.9	-2.2	-9.1	-7.6
Dioxole Formation; w and w/o Spectator Catalysis (TS_d, $TS_{d,cat}$)						
a-c-MVK-oxide = Dioxole	14.4	13.6	14.6	-0.3	14.4	15.2
a-c-MVK-oxide…FA = Dioxole…FA	-0.0	-0.6	2.2	0.7	3.0	4.2
a-c-MVK-oxide…FA = Dioxole…FA Geometry 2	-0.3	-1.3	1.8	0.9	2.6	3.8
Product OO Fission (HPBD)						
s-t-HPBD…FA = OBD…OH…FA; *syn-trans*	-0.1	0.5	-5.9	-1.1	-7.0	-5.5
Products						
HPBF Adduct; optimized	-33.0	-30.8	-33.0	2.8 (2.6)	-30.3	-28.8
s-t-HPBF Adduct	-31.5	-29.2	-31.4	2.8	-28.6	-27.1
s-c-HPBF Adduct	-32.5	-30.3	-32.5	2.8	-29.6	-28.1
a-t-HPBF Adduct	-31.4	-29.2	-31.4	2.8	-28.6	-27.1
a-c-HPBF Adduct	-30.5	-28.4	-30.4	2.6	-27.9	-26.4
ABF + OH	13.7	17.7	16.6	-2.7	13.9	15.4
s-t-HPBD + FA	-8.2	-11.8	-13.1	-0.2	-13.2	-11.7
s-c-HPBD + FA	-9.8	-13.8	-13.8	0.0	-15.0	-13.5
a-t-HPBD + FA	-6.6	-10.0	-11.4	-0.3	-11.7	-10.2
a-c-HPBD + FA	-7.2	-10.9	-12.5	-0.2	-12.8	-11.3
SOZ	-29.6	-25.8	-30.4	3.7	-26.8	-25.3
SOZ; Geometry 2	-30.9	-24.4	-31.8	3.6	-28.2	-26.7
OBD + FA + OH	11.5	11.7	10.4	-5.2	5.8	7.3
OBD…FA + OH	-0.8	-2.1	-0.8	-3.7	-4.5	-3.0

OBD…OH + FA						2.4[e]
c-HPBD-2 + FA	3.9	1.3	0.7	-0.8	-0.1	1.4
t-HPBD-2 + FA	4.6	2.3	1.6	-0.9	0.8	2.3
Dioxole + FA	-26.1	-25.0	1.3	-26.9	-25.6	-24.1

[a] All energies are relative to *syn,trans*-MVK-oxide + OCHOH. The first three columns are electronic energies, the next is the zero-point vibrational energy. The last two columns are the sum of the CCSD(T)-F12/cc-pVTZ-F12 electronic energy and B2PLYP-D3/cc-pVTZ zero-point without and with the ad hoc correction for multireference effects.
[b] Zero-point energies from harmonic B2PLYP-D3/cc-pVTZ calculations. The numbers in parentheses are for the reaction with deuterated FA.
[c] Total corresponds to the sum of the CCSD(T)-F12b energy and E0. [d] The total energy corrected by estimated CCSDT(Q) higher level corrections as discussed in the text of the supplementary material.
[e] From Ref. 5.

Table S2. Stationary point energies (kcal mol^{-1}) for the formic acid catalyzed isomerization of *syn-trans*-MVK-oxide. Energies include ZPE corrections and are reported relative to reactants.

Species	**This work** [a] CCSD(T)-F12/ cc-pVTZ-F12	**This work** [b] CCSD(T)/aug-cc-pVTZ	**Kumar *et al.*** [c] CCSD(T)/aug-cc-pVTZ
MVK-oxide + FA	-14.3	-16.0	-20.5
TS2	-3.8	-6.5	-11.1
HPBD…FA	-21.5	-23.6	-27.0
HPBD + FA	-13.8	-12.9	-11.8

a. CCSD(T)-F12/cc-pVTZ-F12//B2PLYP-D3/cc-pVTZ with estimated CCSDT(Q) corrections.
b. CCSD(T)/aug-cc-pVTZ//M06-2X/aug-cc-pVTZ.
c. Ref. 3, CCSD(T)/aug-cc-pVTZ//M06-2X/aug-cc-pVTZ.

CCSD(T)-F12/cc-pVTZ-F12 based calculations and the prior CCSD(T)/aug-cc-pVTZ based results are larger than would be expected for these levels of theory (ca. 2.0 kcal mol^{-1}). However, we found that the present CCSD(T)/aug-cc-pVTZ//M06-2x/aug-cc-pVTZ calculations show a roughly constant increase of 4 kcal mol^{-1} compared to the prior report; the origin of this discrepancy is not known. The present CCSD(T)/aug-cc-pVTZ calculations are in much improved agreement with the CCSD(T)-F12/cc-pVTZ-F12 based results.

The reaction coordinates for the interconversion between *syn-trans* and *syn-cis* configurations of MVK-oxide and of MVK-oxide…FA PRC are illustrated in Figure S2. The interaction between MVK-oxide and FA results in an isomerization transition state that lies far below the MVK-oxide + FA asymptote. As a result, the reaction of the *syn-trans* and *syn-cis* conformers effectively occurs through an equilibrated pair of *syn-trans* and *syn-cis* MVK-oxide…FA PRC conformers. Note, however, that this does not imply that the rates and products arising from the *syn-trans* and *syn-cis* conformers will be identical; the *syn-cis* reaction is initiated at the higher energy of the *syn-cis* conformer and this additional energy affects the product distributions (as shown below). The reaction coordinate diagram for the isomerization of *anti-trans* and *anti-cis* configurations (not shown) is similar and so the reaction of the *anti-trans* and *anti-cis* conformers also occurs as an equilibrated pair of *anti-trans* and *anti-cis* MVK-oxide…FA PRC conformers. The barrier to transformation from *syn* to *anti* conformers is high enough (31 kcal mol^{-1})[5] that we do not expect the *syn* to *anti* transformation to be rapid even within the PRCs.

The reaction paths for the two reaction channels of primary interest here – the acid-catalyzed pathway through TS2 to form HPBD with release of FA and the adduct formation pathway through TS3 to form the HPBF adduct– are illustrated for the lowest energy *syn-trans* MVK-oxide conformer in the main text (Figure 4). From this diagram it is clear that both TS2 and TS3 saddle points are submerged below reactants, and so can provide effective channels for low-temperature kinetics. Although TS2 lies considerably higher in energy than TS3, simple inspection of the TS structures does not make it clear which channel is favored entropically. The two channels are predicted to proceed through the same PRC.

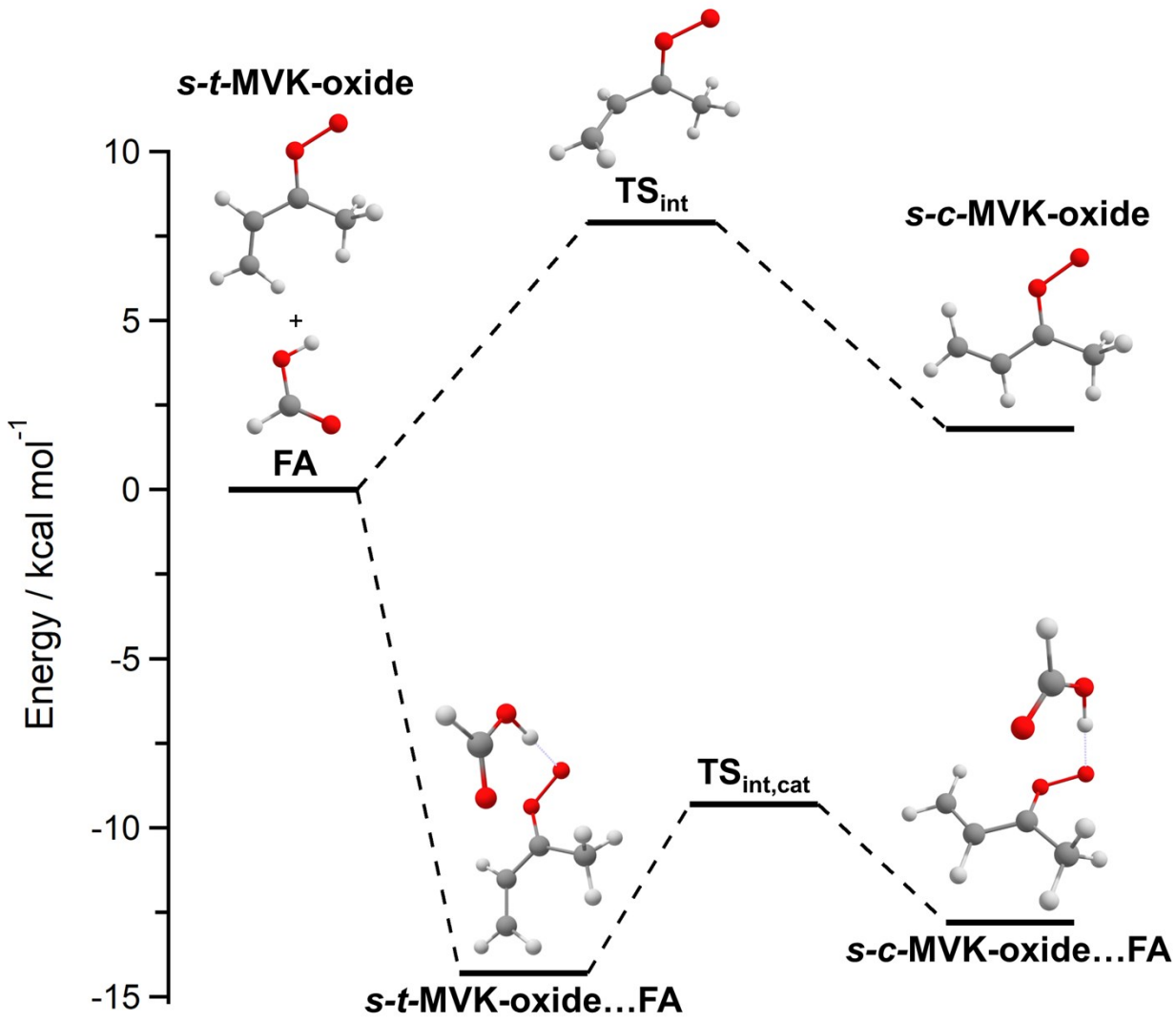

Figure S2. Reaction coordinate showing the barrier (TS_{int}) for interconversion between *syn-trans* and *syn-cis* configurations of MVK-oxide. A pre-reactive complex (PRC) formed between MVK-oxide and formic acid substantially lowers the barrier ($TS_{int,cat}$) and provides a route for rapid interconversion between *trans* (*s-t*) and *cis* (*s-c*) forms.

The process through TS2 directly leads to a complex (HPBD…FA) between HPBD and FA, which is expected to dissociate directly and rapidly to HPBD and FA. Indeed, the master equation calculations find no indication of stabilization of the HPBD…FA complex for any conditions of relevance to atmospheric chemistry. Meanwhile, the dissociation of HPBD to OBD + OH (the lowest bond fission process) is predicted to be endoergic by 7.3 kcal mol^{-1} relative to MVK-oxide + FA reactants. As discussed in Ref. 5, an alternative roaming induced formation of HB (1-hydroxybut-3-en-2-one) has a maximum barrier at only 4.0 kcal mol^{-1} relative to *syn-trans* reactants. This pathway might just be energetically accessible from thermally excited *syn-cis* reactants.

It is interesting to ponder further the possible products that might be formed from the HPBD…FA complex. Notably, a termolecular complex between OBD, OH, and FA is predicted to lie 3.0 kcal mol^{-1} below *syn-trans* reactants. From this complex, which would be formed via partial OO bond fission in HPBD…FA at an energy of -5.5 kcal mol^{-1}, the loss of OH to form OBD…FA + OH has an asymptotic energy of 2.4 kcal mol^{-1}. Meanwhile, the maximum barrier for the roaming isomerization to HB…FA would likely also be weakly submerged. Lastly, the loss of FA to form OBD…OH + FA would have an energy of 2.4 kcal mol^{-1}. However, it seems unlikely that any of these processes would be competitive with the simple loss of FA from the HPBD…FA complex, which occurs at a much lower energy (-13.5 kcal mol^{-1}) and should also have the highest entropy.

The likely lowest energy bond fission for the HPBF adduct (OO fission as in the CH_2OO + FA case[4]) lies at 15 kcal mol^{-1} relative to *syn-trans* MVK-oxide + FA. We expect that the lowest energy molecular eliminations involve CH_3OH and CH_2CHOH loss as analogues of the H_2O loss channel explored for the CH_2OO case.[4] We have not explored these here as we do not expect them to be energetically accessible.

Figure S3 provides a corresponding illustration of these same two reaction paths (TS2 and TS3 analogues) for the reaction of the *anti-trans* MVK-oxide conformer with FA. The reaction path energies are remarkably similar to those for the *syn-trans* case, with the most significant difference being that TS2 for the acid catalysis pathway is not as deeply submerged (-1.0 vs -4.1 kcal mol^{-1}, where both are

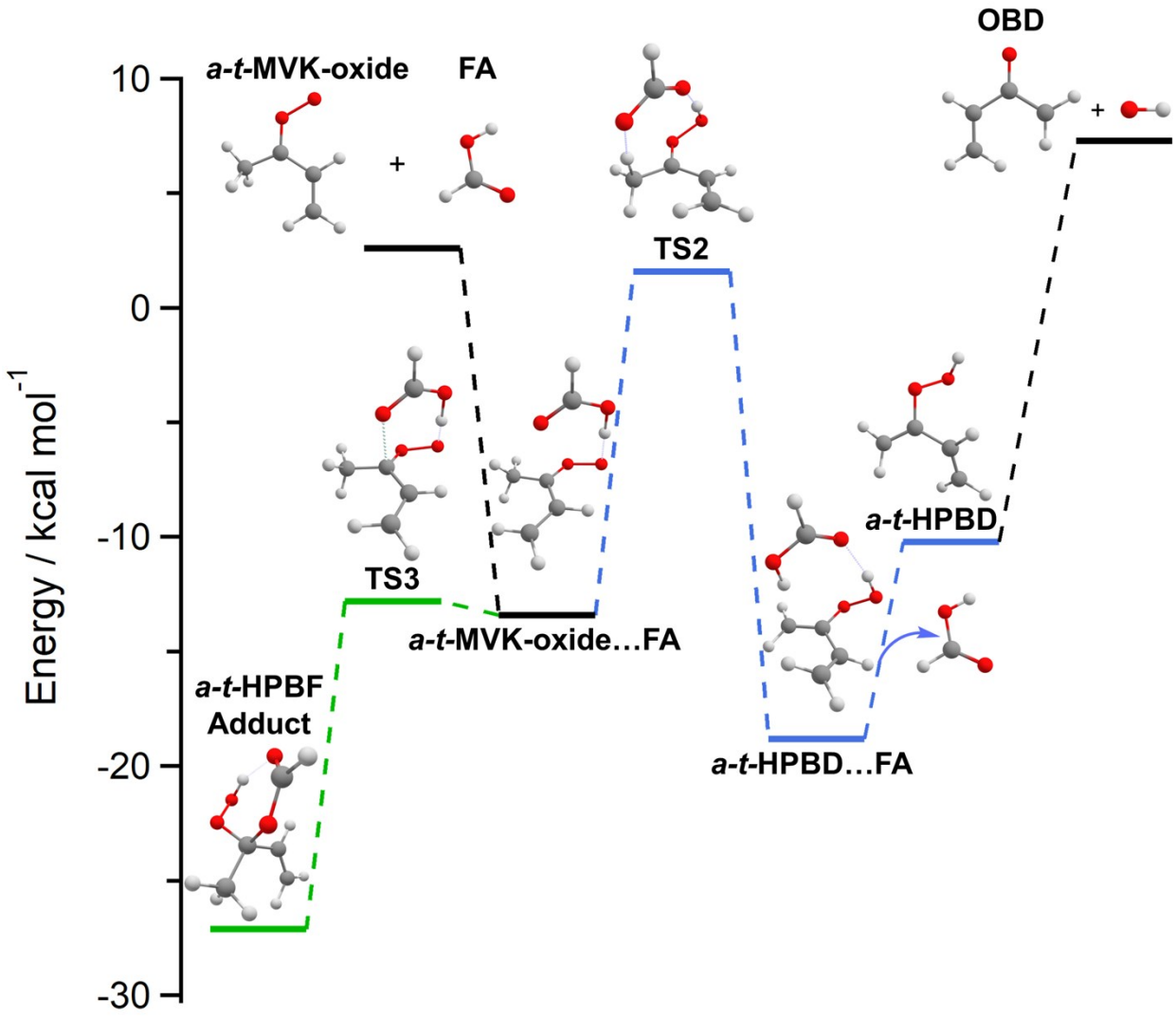

Figure S3. Reaction coordinates showing the formic acid catalyzed isomerization of *anti-trans*-MVK-oxide (blue) and the more favorable adduct formation pathway arising from the 1,4-insertion reaction of *anti-trans*-MVK-oxide with formic acid (green) at the CCSD(T)-F12/cc-pVTZ-F12 //B2PLYP-D3/cc-pVTZ level of theory with estimated CCSDT(Q) corrections (Table S1).

specified relative to their respective reactants). Thus, we expect the branching through this channel to be much smaller than that for *syn-trans*.

For isolated *anti-cis* MVK-oxide, the dominant reaction pathway involves electrocyclic ring closure to yield dioxole. The reaction coordinate diagram provided in Figure S4 demonstrates that, even with the spectator catalytic lowering of the barrier, the barrier for this process is endoergic (by 1.0 kcal mol^{-1} relative to *anti-cis* MVK-oxide reactants) and not competitive with the HPBF adduct formation pathway. The acid catalyzed isomerization of *anti-cis*-MVK-oxide to HPBD is also more favorable than spectator catalysis yielding dioxole.

For *anti-trans* MVK-oxide + FA, an alternative chemical catalysis pathway would involve an H transfer from the vinyl group to the FA. However, as illustrated in Figure S5, this catalytic pathway is not competitive with the catalytic pathway involving H transfer from the methyl group. Thus, the reaction of the *anti* conformers of MVK-oxide with FA should predominantly yield the HPBF adduct (Figure S4) with secondary production of an acid-catalyzed HPBD product as for the *syn* conformers (Figure S5).

Vereecken also found that a 1,2 insertion pathway[4] (where the OH group of FA inserts across the COO moiety in the CI) is slightly submerged (i.e. at -2.4 kcal mol^{-1}). As illustrated in Figure S6, for *syn-trans* MVK-oxide the analogous 1,2 insertion pathway is predicted to be slightly endoergic (1.4 kcal mol^{-1}) and is thus not expected to play a significant role in the kinetics. Vereecken also explored a cyclo addition process to yield a primary ozonide, which was submerged by 1.7 kcal mol^{-1}. As illustrated in Figure S7, for *syn-trans* MVK-oxide the analogous secondary ozonide (SOZ) forming process is highly endoergic, with a predicted barrier of 6.2 kcal mol^{-1}. These increased barrier heights for MVK-oxide relative to CH_2OO are largely the result of the need to break the resonance between the vinyl π bond and the COO π bond prior to bond formation. The extra resonance stabilization in MVK-oxide also leads to decreased bond strengths for the complexes formed. Tables S3-S5 provide a comparison of the reaction pathway energies for the reaction of FA with CH_2OO and *syn-trans* MVK-oxide.

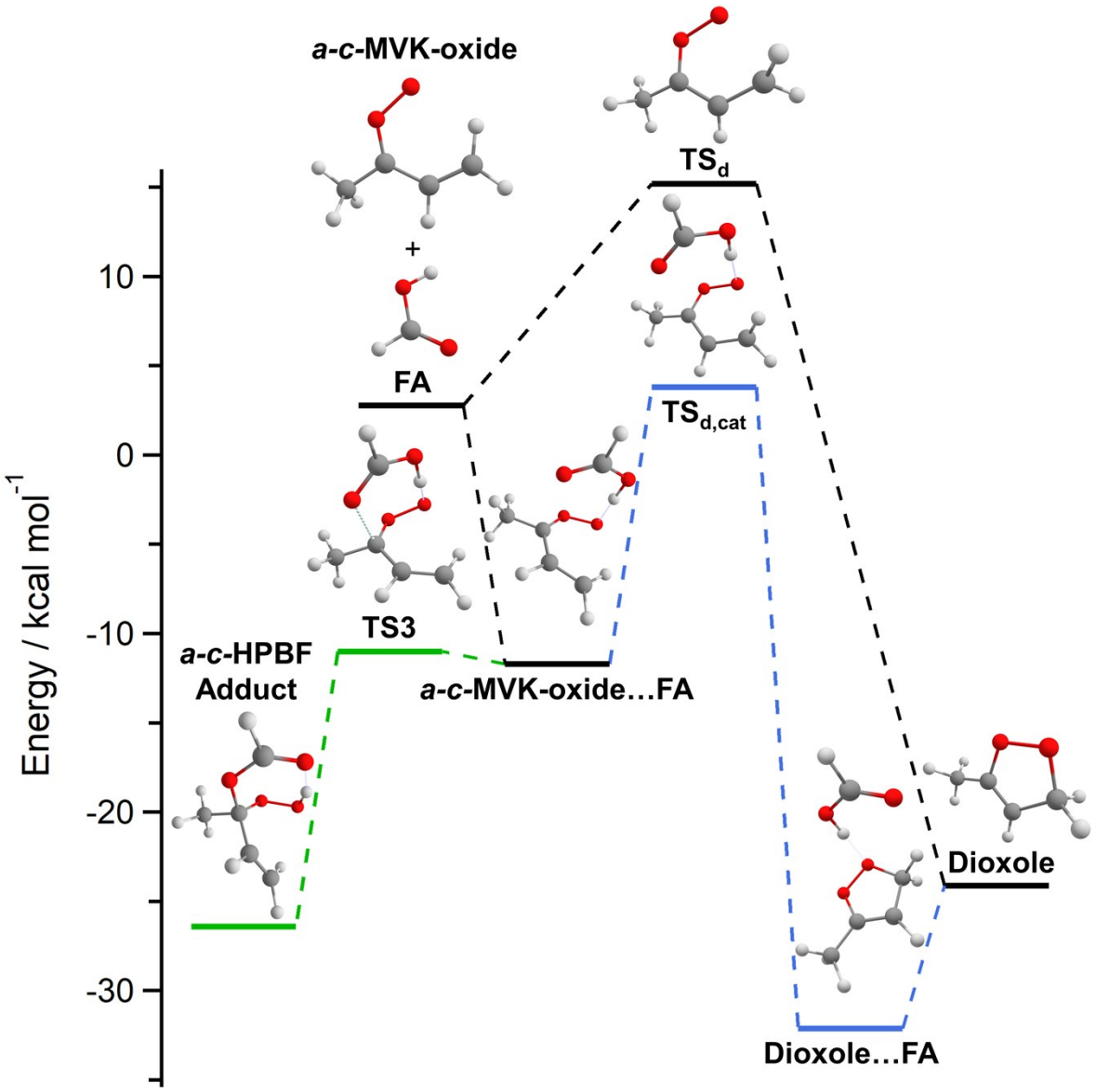

Figure S4. Reaction coordinate for electrocyclic ring closure of *anti-cis*-MVK-oxide to dioxole (black) compared to that for the formic acid spectator catalyzed pathway to dioxole (blue). Also shown is the energetically favorable adduct formation pathway (green) for the *anti-cis*-MVK-oxide + formic acid reaction. Energies are reported at the CCSD(T)-F12/cc-pVTZ-F12//B2PLYP-D3/cc-pVTZ level of theory with estimated CCSDT(Q) corrections (Table S1).

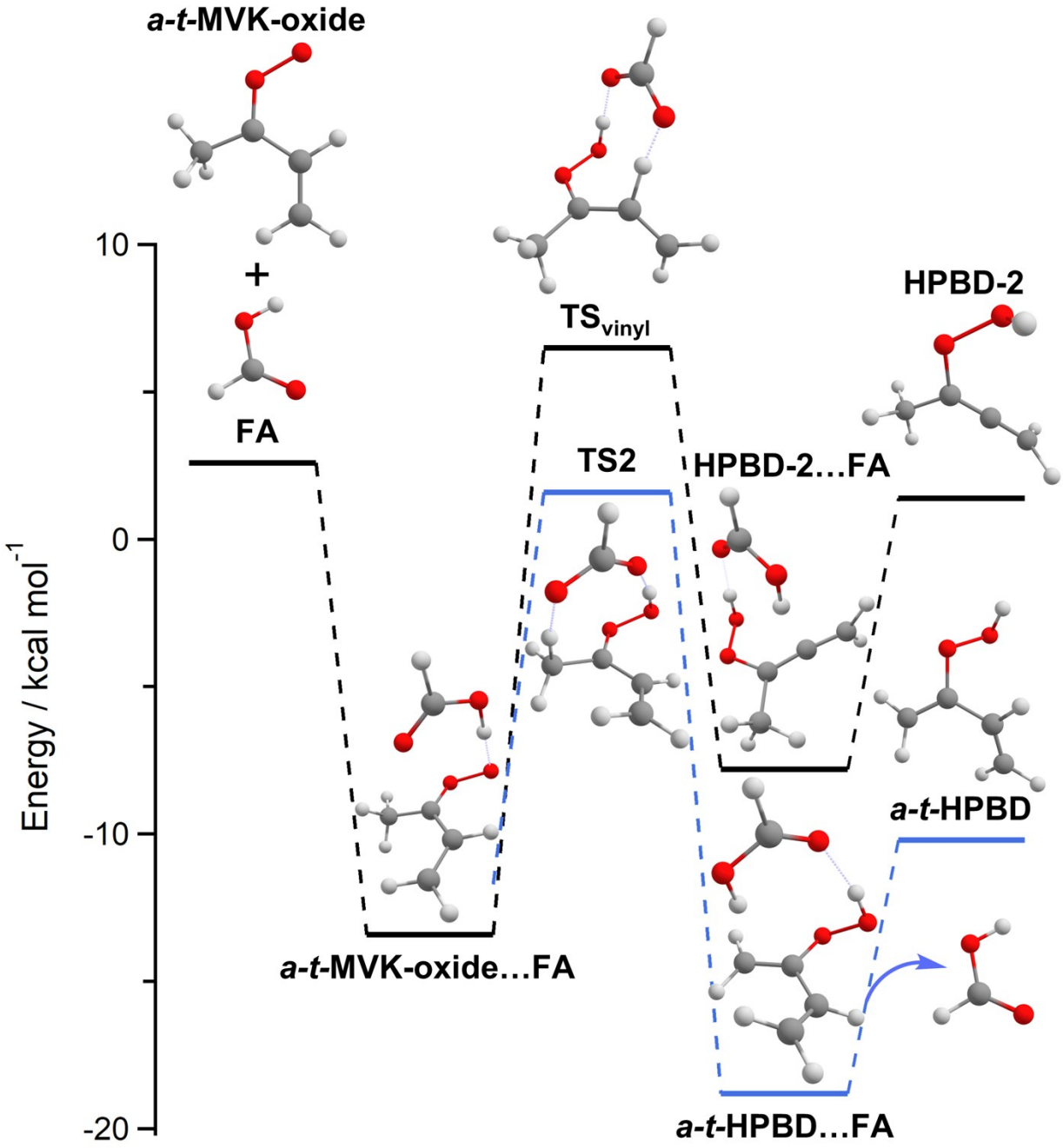

Figure S5. Reaction coordinates comparing different acid catalyzed reaction pathways for the *anti-trans*-MVK-oxide + formic acid reaction. TS2 (blue) and TS_{vinyl} illustrate the barriers for H-atom transfer from the methyl and vinyl group of MVK-oxide, respectively. Energies (Table S1) are determined at the CCSD(T)-F12/cc-pVTZ-F12//B2PLYP-D3/cc-pVTZ level of theory (with estimated CCSDT(Q) corrections) and indicate that the methyl H-atom transfer pathway is more favorable.

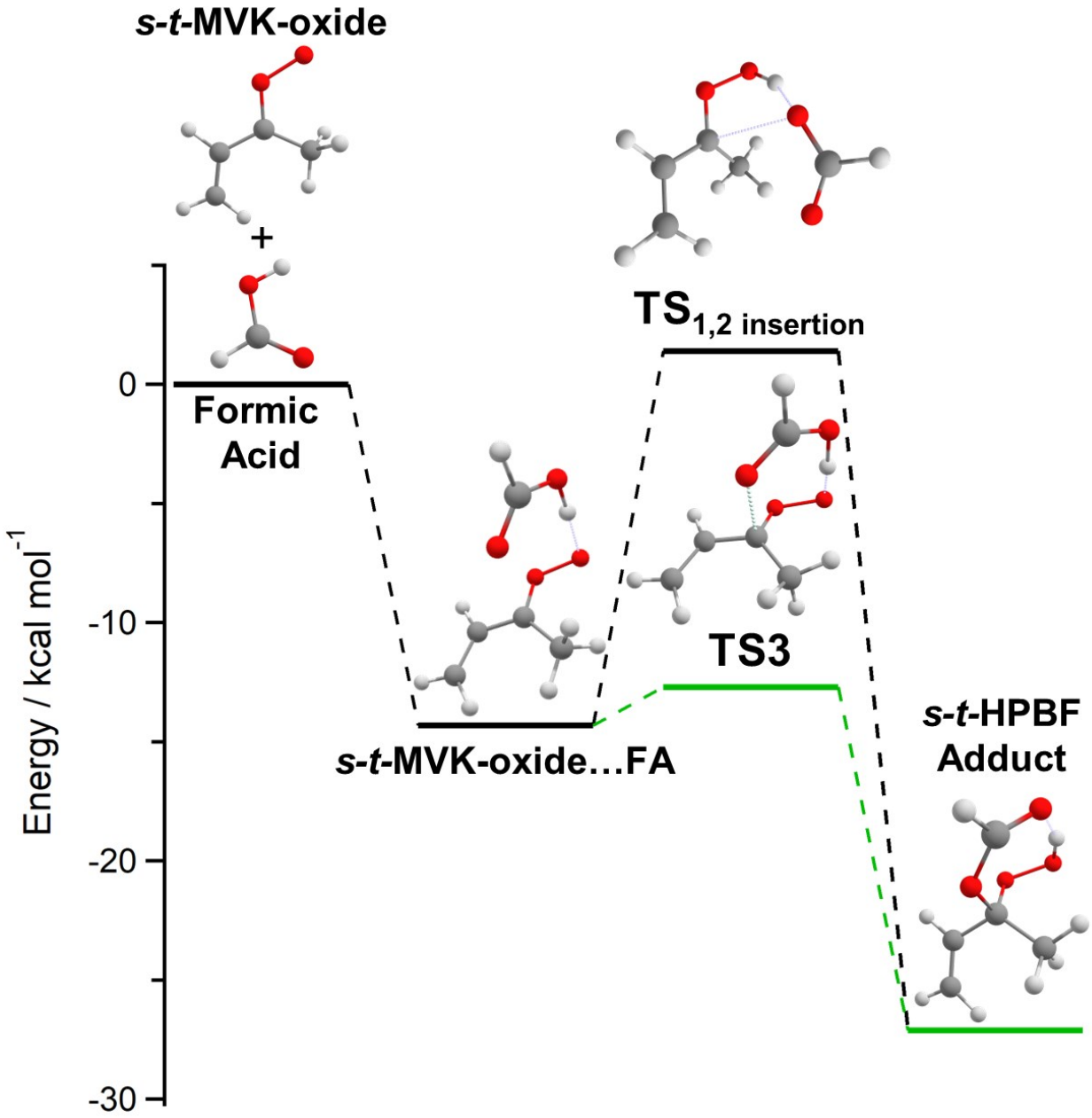

Figure S6. Reaction coordinates comparing adduct formation from the *syn*-MVK-oxide + formic acid reaction via the 1,2-insertion ($TS_{1,2\ insertion}$, black) and 1,4-insertion (TS3, green) mechanisms. Energies are reported at the CCSD(T)-F12/cc-pVTZ-F12//B2PLYP-D3/cc-pVTZ level of theory with estimated CCSDT(Q) corrections (Table S1).

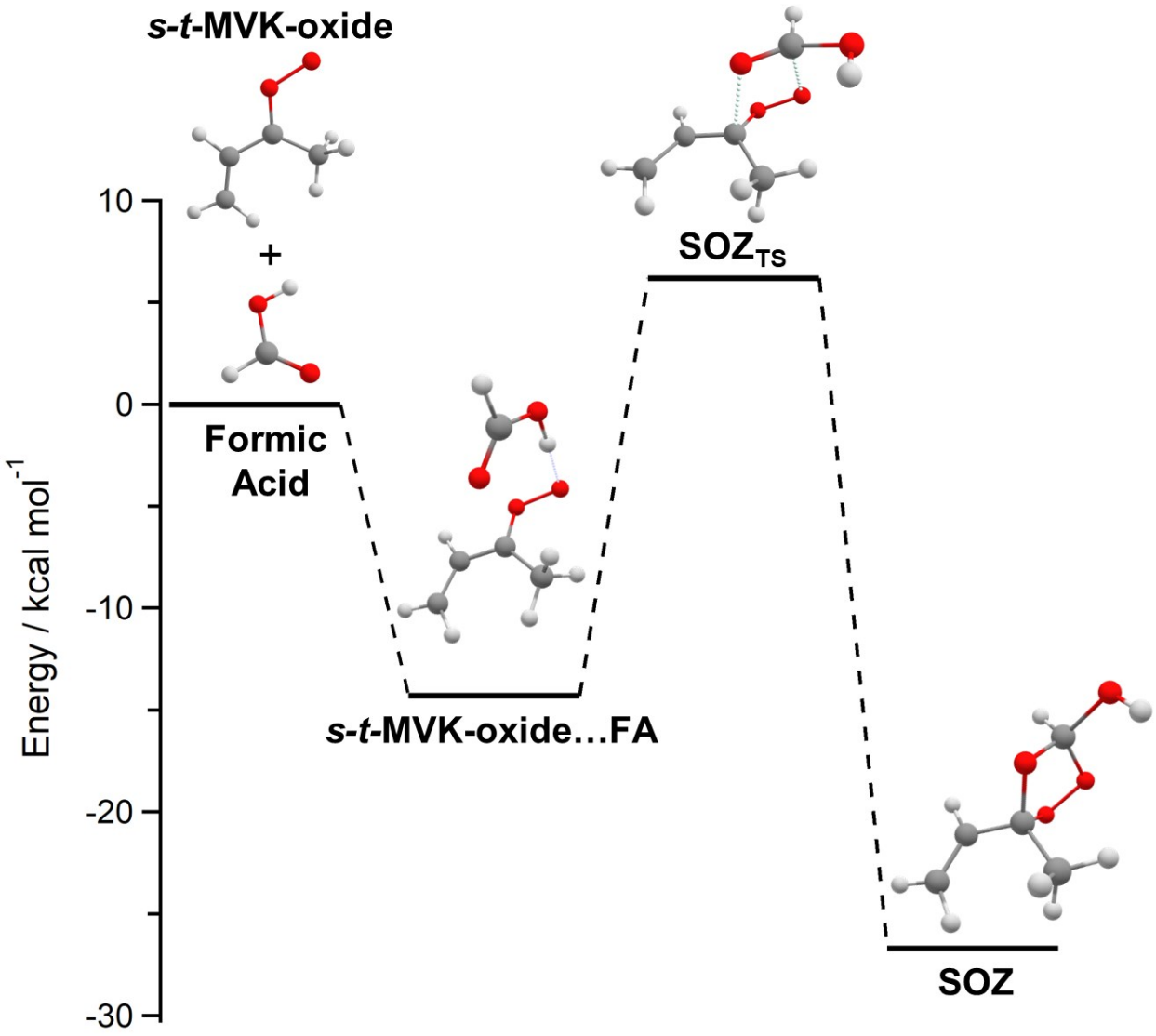

Figure S7. Reaction coordinate showing TS barrier (SOZ_{ts}) to secondary ozonide (SOZ) formation from the *syn*-MVK-oxide + formic acid reaction. Energies are reported at the CCSD(T)-F12/cc-pVTZ-F12//B2PLYP-D3/cc-pVTZ level of theory with estimated CCSDT(Q) corrections (Table S1).

Table S3. Stationary point energies (kcal mol^{-1}) for adduct formation from the reactions of CH_2OO (Vereecken, Ref. 4) and *syn-trans*-MVK-oxide with formic acid via the 1,4-insertion mechanism. Energies include ZPE corrections and are reported relative to reactants.

Species	*syn-trans*-MVK-oxide [a]	CH_2OO [b]
PRC	-14.3	N/A[c]
TS3	-12.7	N/A[c]
HPBF Adduct	-27.1	-44.4

a. CCSD(T)-F12/cc-pVTZ-F12//B2PLYP-D3/cc-pVTZ with estimated CCSDT(Q) corrections.
b. Ref. 4, CCSD(T)/aug-cc-pVTZ//M06-2X/aug-cc-pVTZ.
c. There was no apparent saddle point for the 1,4-insertion mechanism with CH_2OO.

Table S4. Stationary point energies (kcal mol^{-1}) for adduct formation from the reactions of CH_2OO (Vereecken, Ref. 4) and *syn-trans*-MVK-oxide with formic acid via the 1,2-insertion mechanism. Energies include ZPE corrections and are reported relative to reactants.

Species	*syn-trans*-MVK-oxide [a]	CH_2OO [b]
PRC	-14.3	N/A
TS3	1.4	-2.4
Adduct	-27.1	-44.4

a. CCSD(T)-F12/cc-pVTZ-F12//B2PLYP-D3/cc-pVTZ with estimated CCSDT(Q) corrections
b. Ref. 4, CCSD(T)/aug-cc-pVTZ//M06-2X/aug-cc-pVTZ

Table S5. Stationary point energies (kcal mol^{-1}) for SOZ formation from the reaction of CH_2OO (Vereecken, Ref. 4) and *syn-trans*-MVK-oxide with formic acid. Energies include ZPE corrections and are reported relative to reactants.

Species	*syn-trans*-MVK-oxide [a]	CH_2OO [b]
PRC	-14.3	-6.0
TS_{SOZ}	6.2	-1.7
SOZ	-25.3	-40.2

a. CCSD(T)-F12/cc-pVTZ-F12//B2PLYP-D3/cc-pVTZ with estimated CCSDT(Q) corrections
b. Ref. 4, CCSD(T)/aug-cc-pVTZ//M06-2X/aug-cc-pVTZ

For *syn-trans* MVK-oxide in isolation the primary unimolecular decomposition involves an H transfer from the methyl group to the OO group, as studied in detail in Ref. 5. As illustrated in Figure S8, spectator catalysis[6] lowers the isomerization barrier from 18.0 to 7.9 kcal mol^{-1}. Although the barrier is significantly lowered, it is not expected to be an effective kinetic process because of the lower energy channels accessible to the MVK-oxide…FA PRC. The master equation calculations including all the channels validate this expectation.

Although not illustrated here, the reaction pathways for *syn-cis* MVK-oxide reacting with FA closely mimic those for *syn-trans* MVK-oxide. The key kinetic difference is that the rapid equilibration of the *syn-trans* and *syn-cis* PRCs (Figure S2) allows for rapid dissociation of the PRC to *syn-trans* MVK-oxide + FA. Furthermore, the extra 1.8 kcal mol^{-1} conformational energy of the *syn-cis* conformer maps into additional excess energy in the initially formed HPBF adduct. These two effects lower the net adduct formation rate for *syn-cis* relative to *syn-trans* as they both make it harder to stabilize the HPBF adduct. However, in the high-pressure limit, the two rates are predicted to be nearly identical. In the following temperature and pressure dependent kinetic analysis subsection, we explore the extent to which the reactions are occurring in the high-pressure limit via master equation calculations.

As illustrated in Figure S9, the reaction of FA with HPBD can yield H exchange at the hydroperoxyl group. The barriers for the deuterated FA reaction with *syn-cis, syn-trans, anti-cis,* and *anti-trans* HPBD are 4.2. 4.2, 4.2, and 4.7 kcal mol^{-1}, respectively, relative to the respective HPBD + FA asymptotes (Table S6). These barriers are low enough that it seems worth considering the possible ramifications of this process. Thus, we also performed ab initio TST based master equation calculations of the rate constants for this isotopic exchange process (with deuterated FA). There is unlikely to be any direct formation of HPBD from *anti*-MVK-oxide in the photolytic generation process due to the presence of the much lower energy dioxole channel. However, HPBD that might be formed from *syn* conformers in the photolytic preparation of MVK-oxide will likely equilibrate rapidly amongst all four *syn/anti cis/trans* HPBD conformers. Thus, these master equation analyses considered the kinetics for each of the four

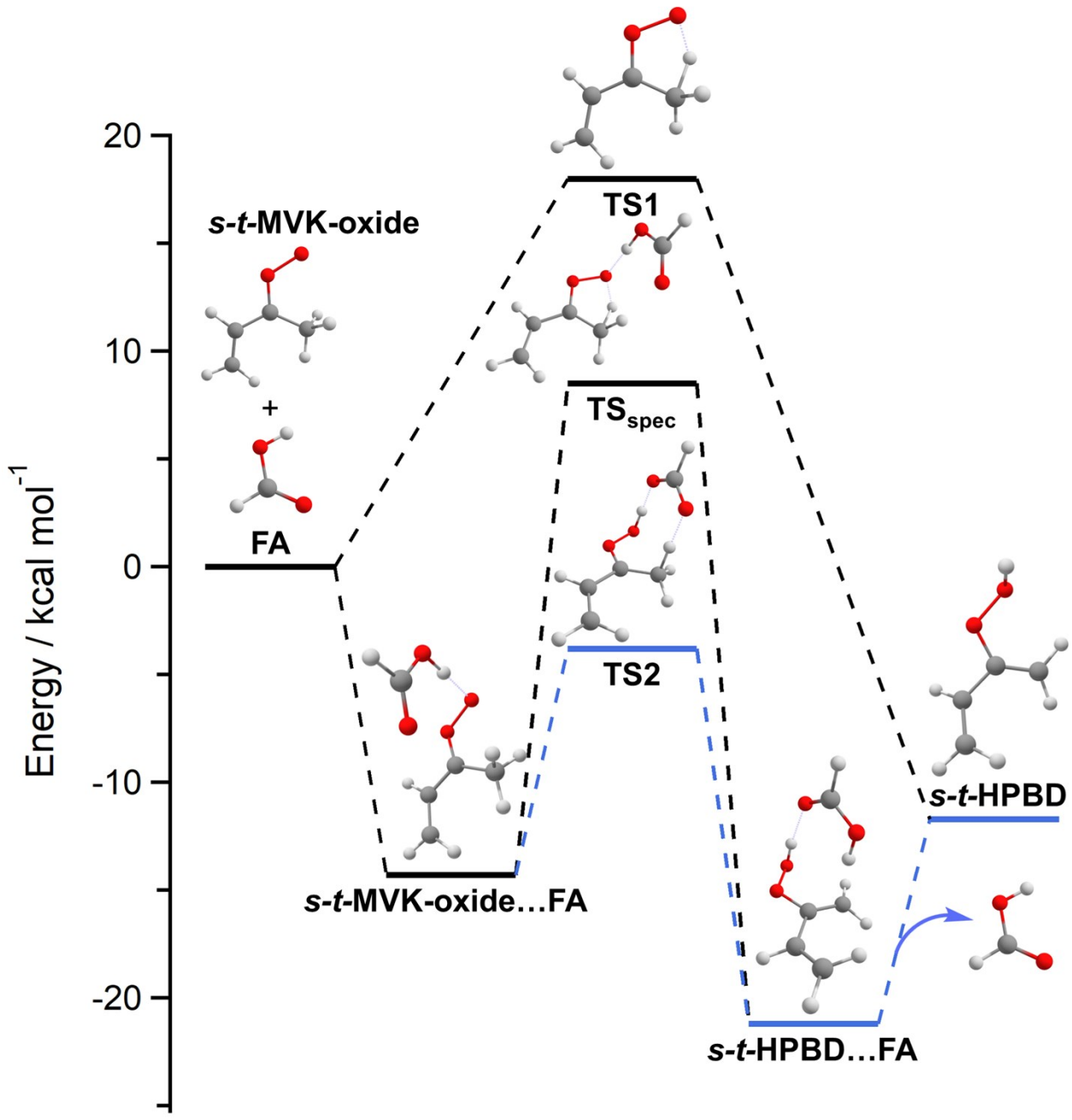

Figure S8. Reaction coordinates showing the chemical catalysis (TS2, blue), spectator catalysis (TS_{spec}), and uncatalyzed isomerization (TS1) pathways for the formation of HPBD from the *syn*-MVK-oxide + formic acid reaction. Energies are from calculations at the CCSD(T)-F12/cc-pVTZ-F12//B2PLYP-D3/cc-pVTZ level of theory with estimated CCSDT(Q) corrections (see Table S1).

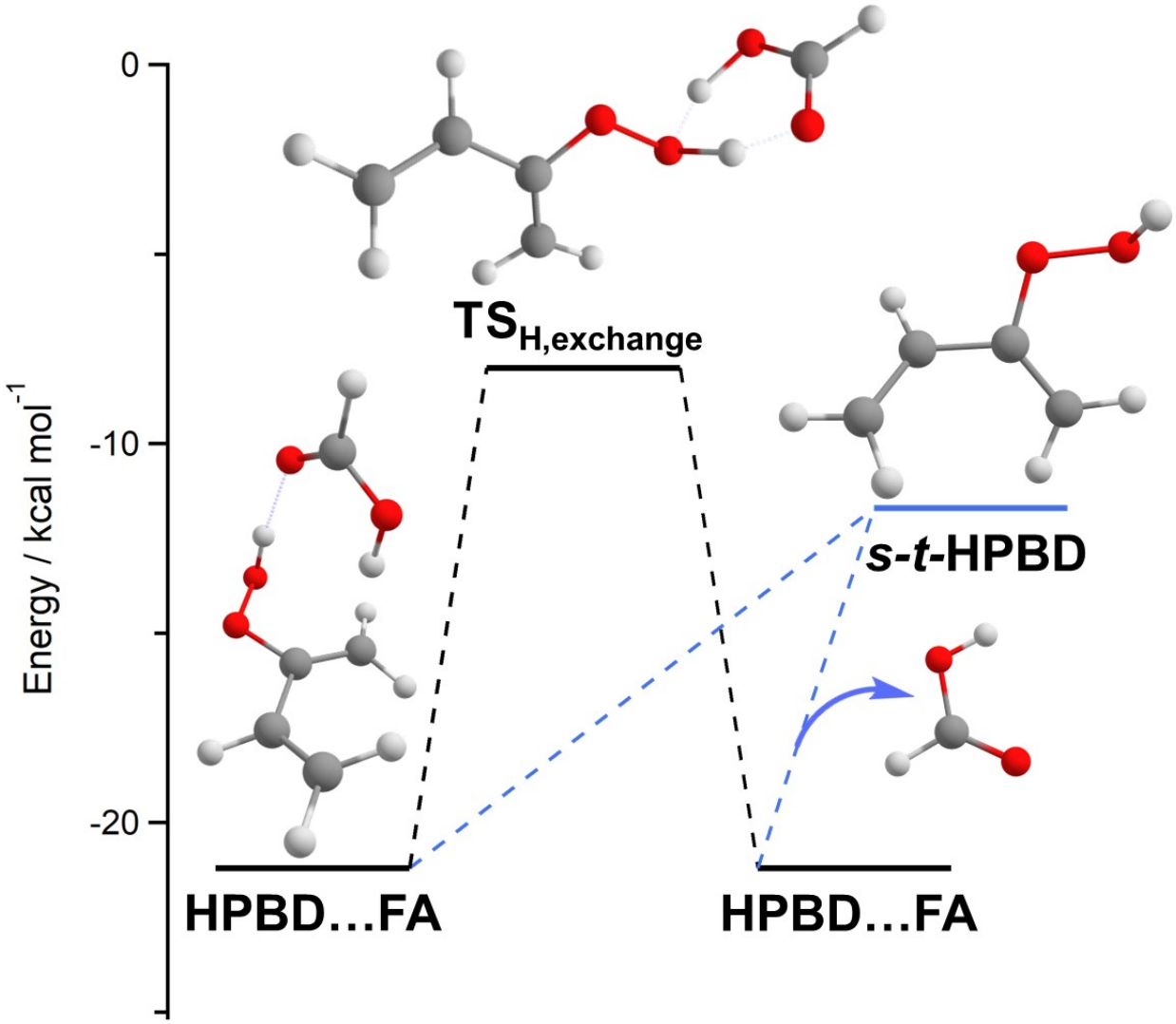

Figure S9. Reaction coordinate for H-atom exchange between the –OOH and –OH functional groups of HPBD and formic acid, respectively. Separation of HPBD and formic acid products is energetically favored compared to H-atom exchange.

Table S6. Stationary point energies (kcal mol^{-1}) for H-exchange in HPBD + FA for both OCHOH and OCDOD isotopes of FA.[a] Energies include ZPE corrections and are reported relative to *syn-cis*-HPBD + FA.

Species	OCHOH	OCDOD
syn-cis-HPBD +FA	0.0	0.0
syn-cis-HPBD…FA	-9.4	-9.5
syn-cis-HPBD…FA = (*syn-cis*-HPBD…FA) exchange	3.7	4.2
(*syn-cis*-HPBD…FA) exchange	-9.4	-9.5
(*syn-cis*-HPBD + FA) exchange	0.0	0.1
syn-trans-HPBD + FA	1.8	1.8
syn-trans-HPBD…FA	-7.7	-7.8
syn-trans-HPBD…FA = (*syn-trans*-HPBD…FA) exchange	5.5	6.0
(*syn-trans*-HPBD…FA) exchange	-7.7	-7.8
(*syn-trans*-HPBD + FA) exchange	1.8	1.9
anti-cis-HPBD + FA	2.3	2.3
anti-cis-HPBD…FA	-5.2	-5.1
anti-cis-HPBD…FA = (*anti-cis*-HPBD…FA)exchange	6.0	6.5
(*anti-cis*-HPBD…FA) exchange	-5.2	-5.4
(*anti-cis*-HPBD + FA) exchange	2.3	2.4
anti-trans-HPBD + FA	3.3	3.3
anti-trans-HPBD…FA	-5.7	-5.8
anti-trans-HPBD…FA = (*anti-trans*-HPBD…FA) exchange	6.5	7.0
(*anti-trans*-HPBD…FA) exchange	-5.7	-5.8
(*anti-trans*-HPBD + FA) exchange	3.3	3.4
syn-cis-HPBD…FA = *syn-trans*-HPBD…FA	-4.7[b]	-4.7[b]
(*syn-cis*-HPBD…FA) exchange = (*syn-trans*-HPBD…FA) exchange	-4.7[b]	-4.9[b]
anti-trans-HPBD…FA = *anti-cis*-HPBD…FA	-0.4[b]	-0.4[b]
(*anti-trans*-HPBD…FA) exchange = (*anti-cis*-HPBD…FA) exchange	-0.4[b]	-0.5[b]
syn-trans-HPBD…FA = *syn-cis*-HPBD…FA	-1.0[b]	-1.1[b]
(*syn-trans*-HPBD…FA) exchange = (*anti-trans*-HPBD…FA) exchange	-1.0[b]	-1.1[b]

a. CCSD(T)-F12/cc-pVTZ-F12//B2PLYP-D3/cc-pVTZ energies with B2PLYPD3/cc-pVTZ ZPE.
b. B2PLYP-D3/cc-pVTZ energies and ZPE.

conformers and included the transition states for interconversion between them. There is little variation in the isotopic exchange reaction paths for the different HPBD conformers.

Temperature and Pressure Dependent Kinetics

Predictions for the thermal rate constants for the reaction of MVK-oxide with FA are obtained from *ab initio* transition state theory-based master equation calculations. In this master equation model, we employ standard exponential down energy transfer probabilities with a temperature dependent expression for the average downwards energy transferred given by $<\Delta E_{down}> = 400\ (T/298)^{0.85}\ cm^{-1}$ and Lennard-Jones collision rate appropriate for He. The increased value for ΔE_{down} employed here (400 vs 300 cm^{-1} in Ref. 2) is likely a better estimate for a molecule the size of the HPBF adduct with 9 heavy atoms.[7] The majority of the calculations were performed for reaction with normal FA (H_2-formic acid). However, sample calculations were also performed to explore the effect of deuteration on the predicted branching.

The requisite partition functions were largely evaluated as discussed in Ref. 2. This mostly involves fixed transition state assumptions employing rigid-rotor harmonic oscillator approximations coupled with hindered rotor treatments of the torsional motions as appropriate. For the HPBF adduct, whose stabilization is central to understanding the temperature and pressure dependence of the kinetics, we include one dimensional hindered rotor representations for all 6 hindered rotor modes. For the other stationary points, the hindered rotor analyses are largely restricted to treatments of the methyl rotor. The vinyl rotor is treated in the harmonic oscillator limit in order to retain a distinction between *cis* and *trans* conformers. The present calculations also include Eckart tunneling corrections for each of the transition states. However, since the key barriers are submerged relative to reactants, simply neglecting tunneling has a minimal (~10%) effect on the predicted branching.

For the entrance channel, which is the primary flux bottleneck for the overall reaction, we employ a VRC-TST analyses with a center-of-mass reaction coordinate to predict the rate of forming the MVK-oxide…FA PRC. This ωB97XD/6-31+G* direct sampling based VRC-TST analyses was implemented

here for all four (*syn-trans*, *syn-cis*, *anti-trans*, and *anti-cis*) conformers of MVK-oxide interacting with FA. A dynamical correction factor of 0.85, based on earlier related reference comparisons of trajectories and TST, is applied to these VRC-TST results. For the conversion from the PRC to the HPBF adduct as well as the other conversions, we now employ fixed transition states. The additional variational components of the treatments described in Ref. 2 for the PRC to HPBF adduct conversion yield only a 10% reduction in the *syn-trans* rate at the conditions of the present experiment. Variational effects are expected to be similar for the other channels. Thus, the present restriction to fixed TST analyses for these conversion steps was deemed appropriate. The interaction energies in the VRC-TST analyses were evaluated via direct sampling of ωB97XD/6-31+G* energies.

As illustrated in Figure S10 and S11, the estimated branching to HPBD + FA (i.e., the acid catalyzed isomerization products) is quite sensitive to both temperature and pressure and is quite a bit larger (~ a factor of four) for the *syn-cis* MVK-oxide reactant than that for the *syn-trans* reactant. TS2 provides the primary bottleneck for acid-catalyzed formation of HPBD and release of FA. In contrast, the rate for forming the HPBF adduct is primarily determined by the rate for forming the MVK-oxide…FA PRC coupled with the probability of stabilization of the HPBF adduct rather than redissociation back to reactants. Also, note that we see no indication of stabilization of the MVK-oxide…FA PRCs under the experimentally relevant ranges of temperature and pressure. Thus, the branching to HPBD + FA is essentially an indication of the competition between passage through TS2 and stabilization of the HPBF adduct.

Interestingly, the increase in the branching for the *syn-cis* reactant is partly due to a rapid equilibration of the *syn-trans*…FA and *syn-cis*…FA PRCs. This equilibration allows the *syn-cis* reactants to proceed through the *syn-trans* TS2 bottleneck, which is 5.9 kcal mol^{-1} below the *syn-cis* reactant asymptote, rather than the *syn-cis* TS2 bottleneck, which is 5.6 kcal mol^{-1} below the *syn-cis* reactant asymptote. In contrast, the *syn-trans* TS2 barrier is only 4.1 kcal mol^{-1} below the *syn-trans* reactant asymptote. This additional excess energy allows the process through TS2 to more effectively compete

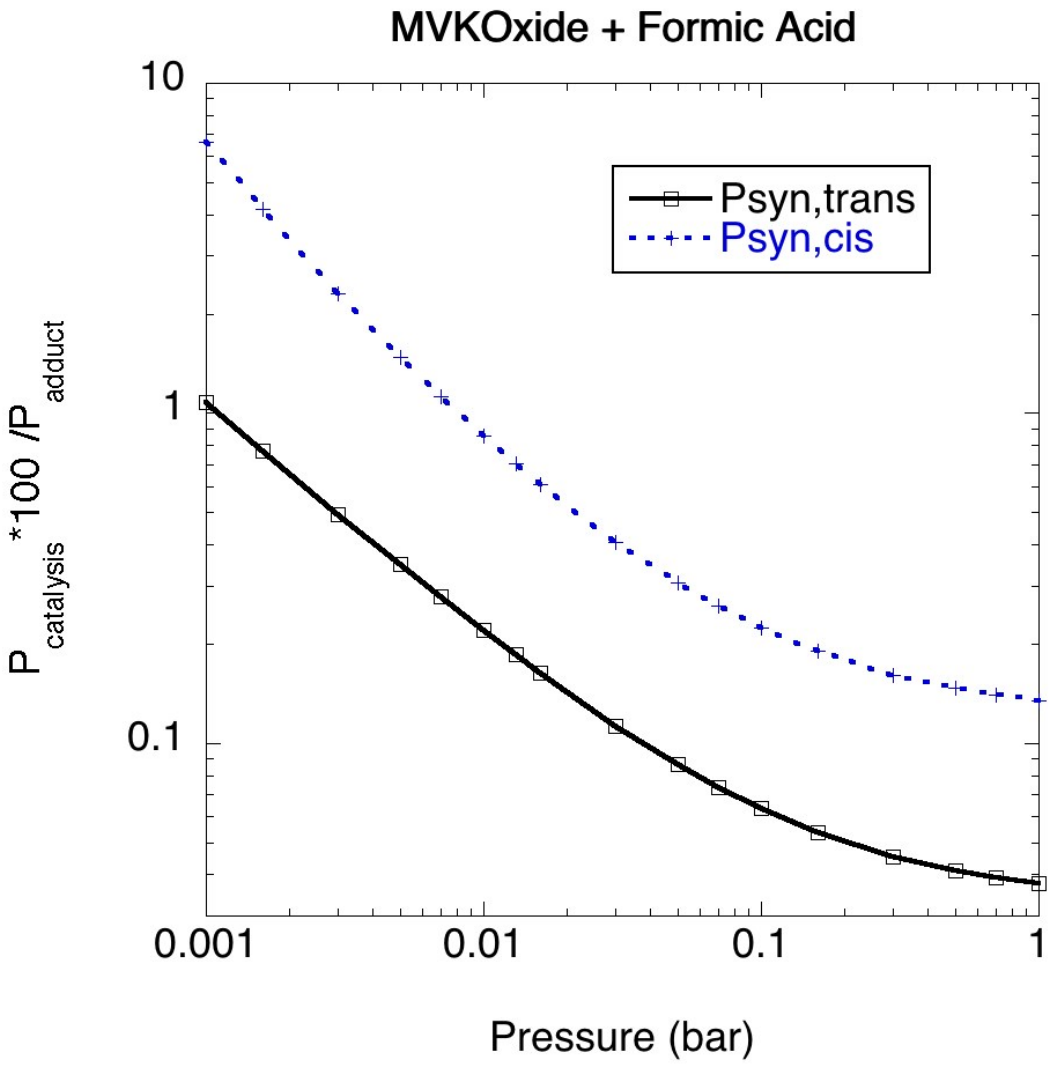

Figure S10. Plot of the pressure dependence for the predicted branching between the acid catalyzed reaction, yielding HPBD with regeneration of formic acid, and chemical adduct formation, yielding the HBPF adduct, in the reaction of *syn-trans* (black solid line) and *syn-cis* (blue dashed line) MVK-oxide with formic acid at 300 K.

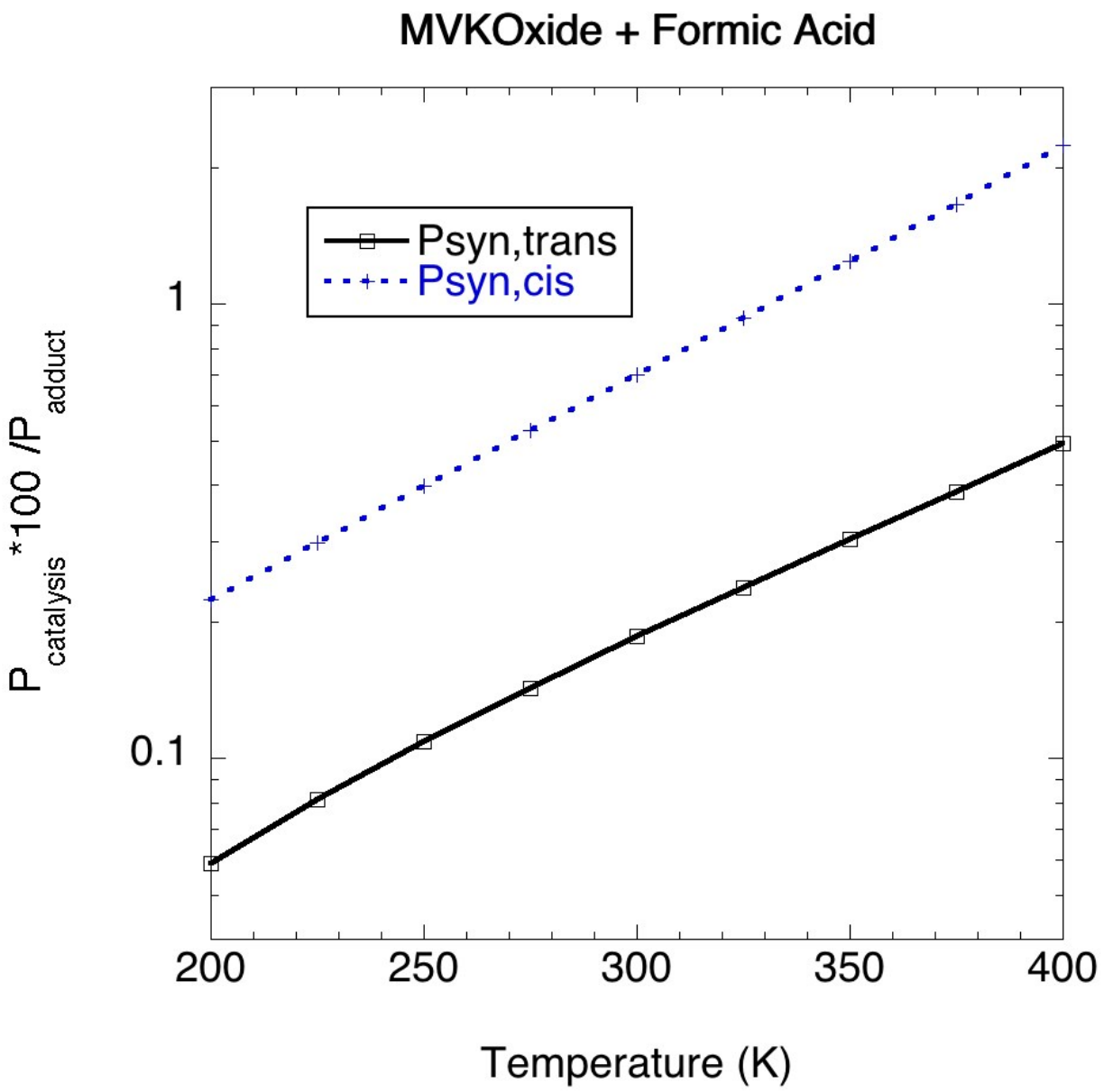

Figure S11. Plot of the temperature dependence of the predicted branching between acid catalyzed reaction, yielding HPBD with regeneration of formic acid, and chemical adduct formation, yielding the HBPF adduct, in the reaction of *syn-trans* (black solid line) and *syn-cis* (blue dashed line) MVK-oxide with formic acid at 1 bar.

with the other processes. Meanwhile, the same increased excess energy also makes it more difficult for the HPBF adduct to be stabilized.

The predicted branching for the acid catalyzed path to HPBD with release of FA is 2-3 orders of magnitude lower for the *anti-cis* and *anti-trans* MVK-oxide compared to *syn*-MVK-oxide with FA. This reduction is largely due to the increased energies of the TS2 saddle points (-1.0 and 1.7 kcal mol^{-1}) relative to their asymptotic reactant states. For the experimentally studied condition of room temperature and a pressure of 10 Torr of He, our reference calculations yield estimated acid catalyzed product branching fractions for the *syn-trans* and *syn-cis* MVK-oxide of 0.19% and 0.70%, respectively. With an estimated equilibrium concentration ratio of *syn-cis* to *syn-trans* of 0.92, the overall branching fraction for the acid catalyzed isomerization is then predicted to be 0.26%. This value is an order of magnitude below that observed experimentally, which ranges from 3-6% depending on the starting *syn/anti* ratio and assuming equivalent photoionization cross sections for the products detected. The latter assumption carries with it considerable uncertainty, with factor of three sorts of deviations in photoionization cross sections amongst related species fairly typical. For example, a recent theoretical study of the photoionization cross sections for ten C1–C4 CIs are about 5 Mb, while those for the corresponding vinyl hydroperoxides (VHPs) are about 20 Mb.[1] If the photoionization cross section for the daughter ions derived from the HPBF adduct was four times that for HPBD, then the present experimental measure of the branching ratio would be 0.8-1.5%, which would be in much better agreement with the theoretical prediction.

We explored the sensitivity of the acid catalysis branching to the uncertainties in various components of the theoretical predictions. The sensitivities reported here are for the experimentally studied condition of room temperature and a pressure of 10 Torr of He. For the most part, these sensitivities are not particularly dependent on conditions for P, T values near these. For simplicity, we report the sensitivities for only the *syn-trans* MVK-oxide reactant; those for the *syn-cis* are similar when considered as multiplicative factor changes. The most significant observation is that lowering the acid catalysis barriers (i.e., TS2 for *syn-trans* and *syn-cis*) by 0.6 kcal mol^{-1}, which is a reasonable estimate of

the uncertainty in this parameter, increases the acid catalysis branching by a factor of 2.1. Similarly, lowering $<\Delta E_{down}>$ by a factor of two, which roughly mimics the uncertainty in the pressure dependence, increases the branching ratio by a factor of 1.9. There is also considerable uncertainty arising from the use of 1D hindered rotors for the torsional modes of HBPF. However, the experimentally observed rate constant from Ref. 2 ($3.0 \pm 0.1 \times 10^{-10}$ cm^3 molecule^{-1} s^{-1}) constrains the extent of the deviations that one can consider for the stabilization rate. For example, the aforementioned decrease in $<\Delta E_{down}>$ by a factor of two also decreases the predicted total reactive rate constant for the *syn-trans* conformer by a factor of 0.75 and for the *syn-cis* conformer by a factor of 0.53. The present total reactive rate constant for the equilibrium mixture of *syn-trans* and *syn-cis* at T = 300 K is 3.1×10^{-10} cm^3 molecule^{-1} s^{-1}, which is essentially identical to the experimental value. Thus, this variation would slightly worsen the agreement for the total rate constant. In contrast, the lowering of TS2 has essentially no effect on the estimated total rate constant. Notably, raising the barrier for formation of the HPBF adduct by 0.6 kcal mol^{-1} has no effect on the branching. An error in the *cis-trans* conformer splitting could also affect the estimated branching ratio. Indeed, shifting the *syn-cis* conformer of MVK-oxide up by 0.5 kcal mol^{-1} increases the predicted catalysis branching ratio for the *syn-cis* reactant by about a factor of 1.6. However, this increased branching ratio is ameliorated by a decreased probability for thermal population of the *syn-cis* conformer.

In summary, the branching to the acid catalysis channel is largely determined by the competition between passage over TS2 and stabilization of the HBPF chemical adduct. Our best theoretical estimate is that this branching is 0.3 %. The above sensitivity analysis suggests that there may be about a factor of four uncertainty in the estimate, with the measured total rate constant providing a strong constraint on the uncertainty in the stabilization rate.

It is perhaps worth emphasizing that the predicted branching fraction is a fairly strong function of temperature (Figure S11). The incipient MVK-oxide suffers numerous collisions with the bath gas prior to reaction, which should cool it to somewhere near room temperature. However, if it was not completely

thermalized the observed branching would be significantly greater. For example, at a temperature of 350 K the *syn-trans* and *syn-cis* branching ratios are factors of 1.6 and 1.8 larger. Furthermore, at 350 K, the equilibrium ratio of *syn-cis/syn-trans* is larger (0.12 vs. 0.08), which yields an effective branching fraction of 0.42. Indeed, with a barrier lowering of 0.6 and a decrease in $<\Delta E_{down}>$ by a factor of two, the predicted branching at 350 K is 1.7, which is within the error bars of the experimental estimate.

The present analysis presumes that the HPBF adduct is a stable product channel. If it were to dissociate on the time scale of the reaction, perhaps via a low barrier process during the initial reaction, then this also would yield an increased value for the predicted catalytic channel branching. However, it seems unlikely that such low energy dissociation channels exist. In addition to these predictions for the reaction of normal FA (H_2-formic acid) with MVK-oxide conformers, we have also predicted the rate constants for fully deuterated FA (D_2-formic acid). Over the experimentally relevant range of conditions, for the *syn-trans* case, the branching ratio is predicted to be a factor of 2-3 lower, while for the *syn-cis* case, it is predicted to be a factor 3 to 4 lower. This smaller predicted branching for the deuterated case arises in part from a 0.4 kcal mol^{-1} increase in the TS2 zero-point correct barriers relative to separated reactants. While the TS3 ZPE corrected point is shifted by an even larger 0.8 kcal mol^{-1}, this barrier plays little role in the HBPF adduct formation rate. Instead, it is largely determined by the stabilization rate, which is significantly increased by the increased rovibrational state densities for the heavier D atoms in deuterated FA.

In summary, although the present prediction for the branching to the catalysis channel is an order of magnitude below the experimentally estimated branching, the uncertainty in this prediction and in its correlation to the experiment is at least a factor of 5 to 10.

Section S3: H/D Exchange

As discussed in main text (Sec. IV), we found evidence of H/D exchange following introduction of D_2-formic acid into the flow cell (Figure S12-S15, Scheme S1, Table S7). Single energy measurements at 11.5 eV (without 248 nm photolysis, 6.4×10^{12} cm^{-3} formic acid) revealed that the D_2-formic acid underwent significant H/D exchange to form D_1-formic acid, yielding a ratio of 1.8:1 of D_2-formic acid (m/z 48) to D_1-formic acid (m/z 47) as shown in Figure S14. We find that H/D exchange occurs mostly at the OD group of D_2-formic acid, producing DC(O)OH, consistent with prior literature.[8-14] Reaction will yield MVK-oxide + D_1-formic acid adducts, which will fragment upon photoionization to form m/z 87 (-DCO_2) and 100 (-HO_2) daughter ions (Scheme S1). The daughter ions (m/z 87) from photoionization of MVK-oxide + DC(O)OH adducts are similar to the daughter ions (m/z 88) from MVK-oxide + D_2-formic acid, the latter of which has a photoionization onset at ca. 10.3 eV (Figure S15).

A portion of the m/z 87 photoionization signal at 10.5 eV arises from daughter ions (-DCO_2) associated with the MVK-oxide + D_1-formic acid adduct. The magnitude of this signal is estimated from the m/z 88 daughter ions (-DCO_2) arising from the MVK-oxide + D_2-formic acid adduct by considering the 1.8:1 ratio of D_2- to D_1-formic acid. The remaining signal on m/z 87 at 10.5 eV is attributed to DPBD. DPBD arising from the D_2-formic acid-catalyzed reaction with MVK-oxide is clearly evident on m/z 87 at lower photoionization energies from 8.7 to 10.2 eV. In addition, MVK-oxide + D1-formic acid will result in HPBD signal on m/z 86, which again is estimated by considering the 1.8:1 ratio of D_2- to D_1-formic acid.

We also considered whether formation of DPBD from isotopic exchange of HPBD with D_2-formic acid might occur, but concluded that this process is unlikely because HPBD formation from thermal unimolecular decay of *syn*-MVK-oxide is slow (33 s^{-1}, 298 K) compared to reaction with formic acid under the experimental conditions (ca. 1900 s^{-1}). Nevertheless, we considered the possibility that our photolytically generated *syn*-MVK-oxide might be sufficiently hot initially (prior to thermalization) to result in more rapid isomerization to HPBD. In this scenario, the initial reactant pool could contain some HPBD as well as MVK-oxide. For this reason, additional electronic structure calculations and master

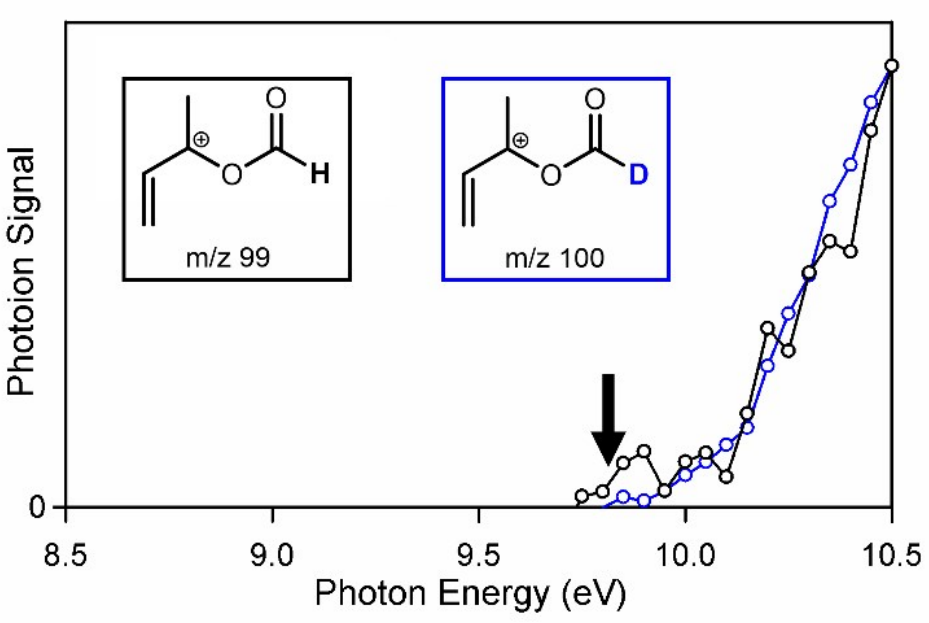

Figure S12. PIE curves of the –H/DO_2 daughter ions (m/z 99 and 100, respectively) from the photoionization of H/DPBF. The photoionization signal is integrated over the full kinetic time window (0-80 ms). The PIE curves are identical and the appearance energies agree well with the adiabatic ionization energy of 9.82 eV (black arrow) computed at an approximate CCSD(T)-F12/cc-pVTZ-F12//B2PLYP-D3/cc-pVTZ level of theory.[2]

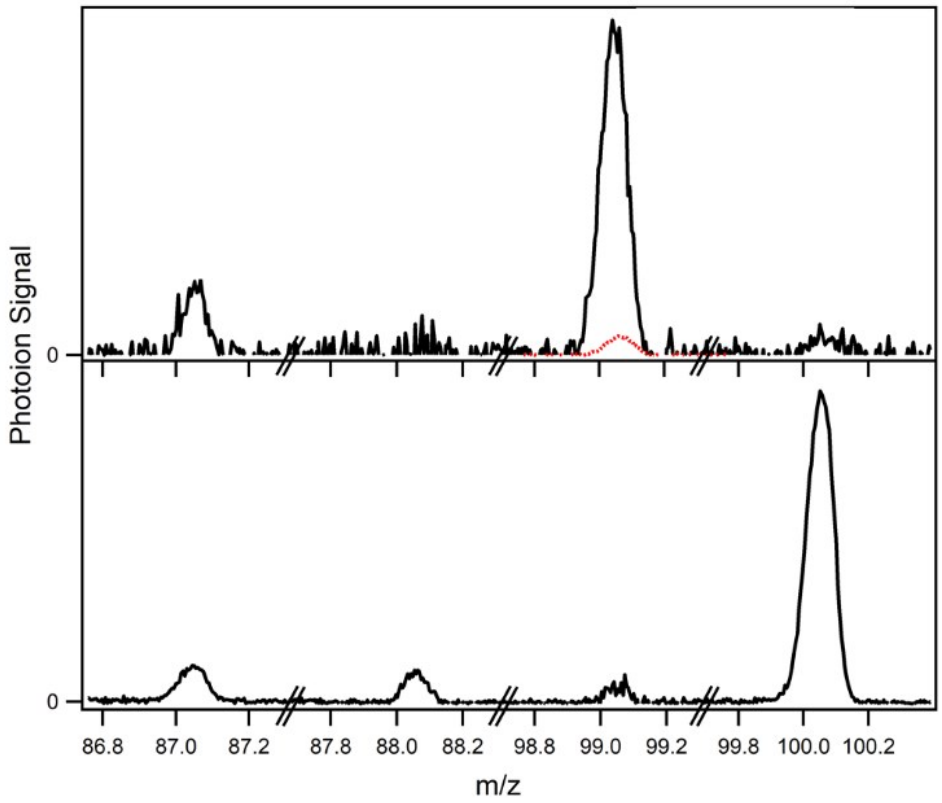

Figure S13. Comparison of relevant features in the mass spectrum obtained from the reaction of MVK-oxide with H_2-formic acid (top panel) and D_2/D_1-formic acid (bottom panel) using MPIMS (10.5 eV, 6.4 × 10^{12} cm^{-3} formic acid). (Top panel) Data reproduced from Caravan et al., *Proc. Natl. Acad. Sci.*, 2020, **117**, 9733-9740 (Ref. 2). Mass channels m/z 87 and 99 appear upon introduction of formic acid and are attributed to $–HCO_2$ and $–HO_2$ daughter ions from the 1,4-insertion product, respectively.[2] The magnitude of the signal on the m/z 100 mass channel is consistent with the natural abundance of ^{13}C associated with the m/z 99 signal (red dashed line). (Bottom panel) Partially deuterated analogs generated from the reaction of MVK-oxide with formic acid (D_2, D_1, and H_2-formic acid). The fractional contribution to each mass channel is shown in Table S7.

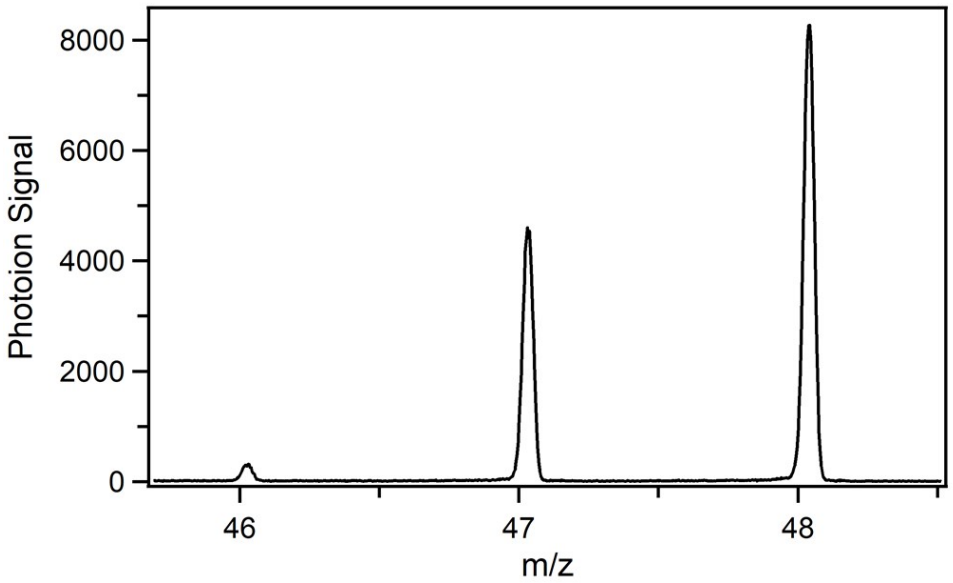

Figure S14. Photoionization signal of D_2-formic acid (m/z 48), D_1-formic acid (m/z 47), and non-deuterated formic acid (m/z 46) obtained with a photoionization energy of 11.5 eV, 6.4×10^{12} cm^{-3} formic acid, and in the absence of 248 nm photolysis.

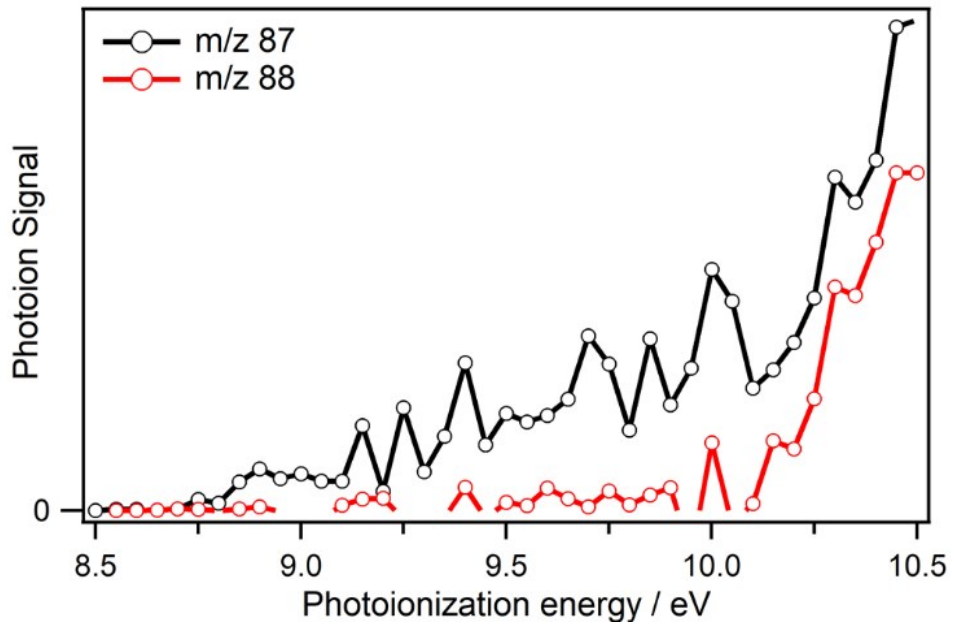

Figure S15. Photoionization efficiency curve of m/z 87 and 88 obtained by integration over the full kinetic time window (0-80 ms) in the reaction of MVK-oxide with D_2-formic acid (6.4×10^{12} cm^{-3}). The m/z 88 PIE curve matches the onset energy and shape of the higher energy component of m/z 87 and is scaled to represent the fraction of the daughter ion contributing to the m/z 87 signal at 10.5 eV (Table S7).

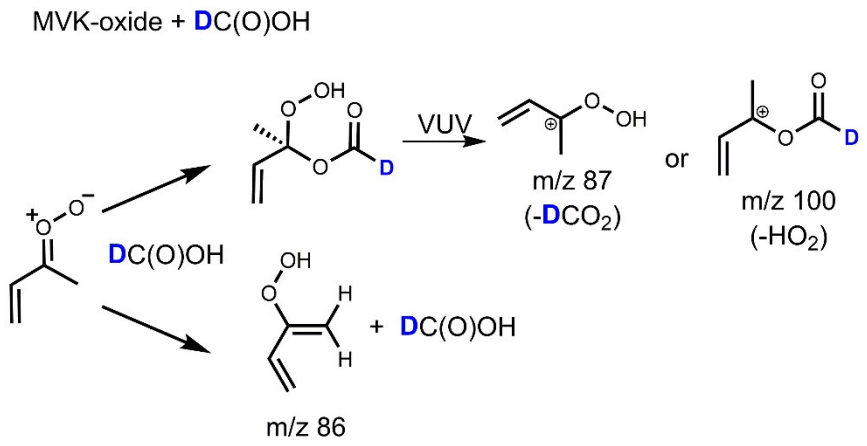

Scheme S1. Products for the reaction between *syn*-MVK-oxide and DC(O)OH (top) and HC(O)OD (bottom) and predicted m/z for the daughter ions formed from the respective adducts.

Table S7. Fractional contributions to the m/z 87, 88, 99, and 100 mass channels from the reaction of MVK-oxide with formic acid (D_2, D_1, and H_2-formic acid) using MPIMS (6.4×10^{12} cm^{-3} formic acid) at 8.5-9.8 eV and 10.5 eV. The isotope of formic acid that reacts with MVK-oxide to yield the corresponding species is given in parenthesis.

Species	Fractional Contribution (8.5-9.8 eV)	Fractional Contribution (10.5 eV)
m/z 87		
Adduct - DCO_2 (D_1-formic acid)	0.00	0.69
DPBD (D_2-formic acid)	1.00	0.27
Adduct - HCO_2 (H_2-formic acid)	0.00	0.04
m/z 88		
Adduct - DCO_2 (D_2-formic acid)	0.00	0.97
C^{13} Adduct - DCO_2 (D_1-formic acid)	0.00	0.02
C^{13} DPBD (D_2-formic acid)	1.00	0.01
C^{13} Adduct - HCO_2 (H_2-formic acid)	0.00	0.00
m/z 99		
Adduct - HO_2 (H_2-formic acid)	0.00	1.00
m/z 100		
Adduct - DO_2 (D_2-formic acid)	0.00	0.64
Adduct - HO_2 (D_1-formic acid)	0.00	0.36
C^{13} Adduct – HO_2 (H_2-formic acid)	0.00	0.00

equation modeling were carried out to assess the isotopic exchange rate of HPBD with D_2-formic acid to form DPBD. As shown in Figure S9, the barrier for isotopic exchange is significant (ca. 4.2 kcal mol^{-1} relative to HPBD + FA for *syn-cis* HPBD) and the associated rate constants (1×10^{-16}, 2×10^{-17}, 1×10^{-16}, and 3×10^{-17} cm^3 s^{-1} for *syn-trans, syn-cis, anti-trans,* and *anti-cis* HPBD reacting with deuterated FA) indicate that isotopic exchange would be negligible on the timescale of the experiment (ca. $2\text{-}6 \times 10^{-4}$ s^{-1}).

Section S4. Stationary point geometries

Structure and Frequencies at the B2PLYPD3/cc-pVTZ level

Reactants

Formic Acid

Ground Conformer

1	8	0	-1.030691	-0.442769	0.000000
2	6	0	0.000000	0.421203	0.000000
3	1	0	-0.650948	-1.334313	0.000000
4	1	0	-0.381240	1.445918	0.000000
5	8	0	1.159715	0.112917	0.000000

Frequencies --	629.6563	686.8589	1062.1848
Frequencies --	1129.9053	1313.9525	1413.8309
Frequencies --	1813.0629	3087.3525	3744.3339

Excited Conformer

1	8	0	1.057366	-0.280350	0.000007
2	6	0	-0.132069	0.361181	-0.000016
3	1	0	1.768925	0.369415	-0.000024
4	1	0	-0.036282	1.457149	0.000043
5	8	0	-1.174895	-0.218856	0.000003

Frequencies --	529.8905	661.3040	1042.0529
Frequencies --	1118.2063	1283.0471	1428.5019
Frequencies --	1857.3853	2996.2484	3813.7007

MVK-oxide

syn-trans-MVK-oxide

1	6	0	-0.281002	-2.428825	0.000000
2	6	0	0.489860	-1.332579	0.000000
3	6	0	0.000000	0.017627	0.000000
4	6	0	-1.397431	0.477385	0.000000
5	8	0	0.934365	0.910720	0.000000
6	8	0	0.561182	2.203583	0.000000
7	1	0	-1.359012	-2.376515	0.000000
8	1	0	0.163693	-3.411629	0.000000
9	1	0	1.567972	-1.424436	0.000000
10	1	0	-2.098829	-0.348501	0.000000
11	1	0	-1.553379	1.122502	0.866535
12	1	0	-1.553379	1.122502	-0.866535

Frequencies --	119.9147	198.1647	256.1167
Frequencies --	283.2193	331.6966	459.4209
Frequencies --	496.8539	609.8350	682.4911
Frequencies --	814.7146	950.8478	998.3597
Frequencies --	1026.7698	1041.7510	1047.8678
Frequencies --	1076.4570	1292.3767	1337.6406
Frequencies --	1400.1620	1449.9665	1453.0141
Frequencies --	1472.8403	1504.9644	1662.0030
Frequencies --	3052.6351	3097.5438	3178.5451
Frequencies --	3186.9118	3194.4379	3270.2727

syn-cis-MVK-oxide

1	6	0	-2.181296	-0.839531	0.000000
2	6	0	-1.445765	0.279851	0.000000
3	6	0	0.000000	0.334288	0.000000
4	6	0	0.795556	1.572979	0.000000
5	8	0	0.625731	-0.789133	0.000000
6	8	0	1.976736	-0.749625	0.000000
7	1	0	-1.722960	-1.817168	0.000000
8	1	0	-3.258737	-0.787750	0.000000
9	1	0	-1.934488	1.244081	0.000000
10	1	0	0.161642	2.453346	0.000000
11	1	0	1.461921	1.566019	0.865256
12	1	0	1.461921	1.566019	-0.865256

Frequencies -- 66.4658 206.2188 228.8220
Frequencies -- 275.2111 327.6923 442.9534
Frequencies -- 485.9721 623.2547 665.9256
Frequencies -- 815.8805 971.1810 992.1262
Frequencies -- 1024.2898 1041.0284 1044.4521
Frequencies -- 1108.3087 1286.3487 1340.7090
Frequencies -- 1397.3938 1418.9712 1451.4392
Frequencies -- 1475.0005 1500.5024 1669.4449
Frequencies -- 3044.5296 3088.3513 3171.9026
Frequencies -- 3177.8055 3200.0465 3272.9201

anti-trans-MVK-oxide

1	6	0	-1.894146	-1.185090	0.000000
2	6	0	-0.571837	-0.965527	0.000000
3	6	0	0.000000	0.349961	0.000000
4	6	0	-0.769734	1.622704	0.000000
5	8	0	1.282506	0.506388	0.000000
6	8	0	2.101575	-0.560185	0.000000
7	1	0	-2.612894	-0.378124	0.000000
8	1	0	-2.286939	-2.190359	0.000000
9	1	0	0.144815	-1.772424	0.000000
10	1	0	-0.083752	2.464487	0.000000
11	1	0	-1.409789	1.687253	0.880050
12	1	0	-1.409789	1.687253	-0.880050

Frequencies -- 113.8309 150.9705 244.3138
Frequencies -- 280.5671 326.0586 377.0466
Frequencies -- 479.0748 640.2948 718.3130
Frequencies -- 798.5875 977.2758 985.0386
Frequencies -- 1021.2924 1049.6643 1057.6112
Frequencies -- 1065.0237 1281.3674 1373.2418
Frequencies -- 1391.3621 1436.2627 1469.0936
Frequencies -- 1486.0836 1512.5356 1657.6094
Frequencies -- 3054.8184 3111.1078 3162.1730
Frequencies -- 3170.5660 3228.1091 3261.6980

anti-cis-MVK-oxide

1	6	0	-1.352990	-1.521124	0.000000
2	6	0	-1.214381	-0.180848	0.000000
3	6	0	0.000000	0.576665	0.000000

4	6	0	-0.021963	2.069054	0.000000
5	8	0	1.191358	0.084982	0.000000
6	8	0	1.382201	-1.251687	0.000000
7	1	0	-0.494812	-2.166647	0.000000
8	1	0	-2.348757	-1.942692	0.000000
9	1	0	-2.104292	0.435798	0.000000
10	1	0	0.990778	2.459965	0.000000
11	1	0	-0.547687	2.442365	0.879064
12	1	0	-0.547687	2.442365	-0.879064

Frequencies --	116.7361	165.5085	285.0024
Frequencies --	305.2060	339.0183	368.0726
Frequencies --	411.2073	640.2272	717.5908
Frequencies --	823.6757	990.3387	1004.8285
Frequencies --	1029.1718	1053.3593	1054.9509
Frequencies --	1099.6379	1269.7395	1340.3444
Frequencies --	1418.9240	1438.3092	1463.9237
Frequencies --	1487.0283	1508.1717	1640.9833
Frequencies --	3054.6683	3110.9627	3165.1107
Frequencies --	3167.2660	3181.8932	3314.1293

van der Waals

Pre-reactive Complex (PRC)

syn-trans-MVK-oxide…FA

1	6	0	0.000000	0.000000	0.000000
2	8	0	0.000000	0.000000	1.275955
3	8	0	1.245775	0.000000	1.892005
4	8	0	0.606398	-2.800437	0.381749
5	6	0	1.017466	-3.231013	1.441733
6	8	0	1.418780	-2.525602	2.475900
7	1	0	1.096188	-4.304566	1.647652
8	1	0	1.354816	-1.531258	2.273211
9	6	0	1.271230	0.075133	-0.735745
10	6	0	-1.329184	-0.043379	-0.564140
11	6	0	-1.585380	-0.054876	-1.875686
12	1	0	1.115967	0.238392	-1.795234
13	1	0	1.804535	-0.859772	-0.570167
14	1	0	1.877193	0.865388	-0.294599
15	1	0	-2.132100	-0.086121	0.158207
16	1	0	-0.802662	-0.028630	-2.617617
17	1	0	-2.601700	-0.103459	-2.234886

Frequencies --	46.8365	56.9407	93.3520
Frequencies --	126.3653	148.3550	156.9454
Frequencies --	221.9254	247.4525	269.3290
Frequencies --	338.2014	358.9841	455.7681
Frequencies --	493.3374	597.9164	688.1404
Frequencies --	708.0896	808.8531	926.4019
Frequencies --	991.7365	1019.5153	1028.1072
Frequencies --	1041.7520	1047.0099	1071.0999
Frequencies --	1116.5869	1260.2678	1313.3572

Frequencies --	1342.3675	1392.1696	1408.1414
Frequencies --	1457.3675	1471.1291	1492.7186
Frequencies --	1502.5265	1519.0126	1678.8845
Frequencies --	1747.2199	2799.5379	3051.0151
Frequencies --	3073.7270	3135.1225	3183.0650
Frequencies --	3193.5201	3207.7761	3275.1933

syn-cis-MVK-oxide…FA

1	6	0	1.132193	0.487665	0.158859
2	8	0	0.487589	0.599430	-0.930436
3	8	0	-0.565686	1.519350	-0.926426
4	8	0	-1.133433	-1.064330	0.956327
5	6	0	-2.204612	-0.979901	0.386149
6	8	0	-2.542801	-0.097738	-0.526240
7	1	0	-3.031630	-1.669855	0.589658
8	1	0	-1.771294	0.547472	-0.701533
9	6	0	0.841254	1.378681	1.293104
10	6	0	2.172951	-0.525711	0.186349
11	6	0	2.254705	-1.523727	-0.697945
12	1	0	1.599302	1.287444	2.063809
13	1	0	-0.134383	1.101857	1.691311
14	1	0	0.749633	2.400404	0.926418
15	1	0	2.872152	-0.453729	1.006188
16	1	0	1.532375	-1.628481	-1.493344
17	1	0	3.039543	-2.260842	-0.627391

Frequencies --	35.9783	50.7715	78.9710
Frequencies --	116.7747	153.3154	153.8978
Frequencies --	211.7184	245.5213	248.6897
Frequencies --	328.7333	358.1968	438.8406
Frequencies --	491.6183	609.4323	663.3595
Frequencies --	711.2670	806.6051	918.5517
Frequencies --	1010.0395	1016.2609	1037.2922
Frequencies --	1038.6597	1049.7664	1105.8282
Frequencies --	1125.9262	1265.2711	1281.1358
Frequencies --	1343.0359	1390.0446	1408.5084
Frequencies --	1455.4723	1457.6423	1500.0159
Frequencies --	1503.4379	1526.5403	1682.5908
Frequencies --	1743.2214	2726.6027	3049.1261
Frequencies --	3066.8455	3130.2559	3177.4779
Frequencies --	3180.3431	3213.5756	3276.5370

anti-trans-MVK-oxide…FA

1	6	0	-1.022369	0.452648	0.256137
2	8	0	-0.201217	1.417145	0.383966
3	8	0	0.623181	1.716719	-0.712649
4	8	0	0.954579	-1.265658	0.680425
5	6	0	2.083787	-1.045449	0.277626
6	8	0	2.502603	0.019599	-0.357573
7	1	0	2.897372	-1.765381	0.420660
8	1	0	1.746193	0.709203	-0.490734
9	6	0	-1.757051	0.111386	1.500844

10	6	0	-1.245512	-0.177821	-1.022322
11	6	0	-2.106148	-1.188613	-1.175042
12	1	0	-1.486192	-0.902416	1.791548
13	1	0	-2.832570	0.157903	1.342765
14	1	0	-1.471195	0.794945	2.293514
15	1	0	-0.680581	0.233483	-1.842294
16	1	0	-2.651151	-1.614467	-0.345551
17	1	0	-2.271295	-1.628631	-2.146727

Frequencies -- 38.2490 81.2065 90.2153
Frequencies -- 114.6818 143.0581 172.2867
Frequencies -- 236.4631 263.1843 267.8510
Frequencies -- 334.8430 361.0513 397.7478
Frequencies -- 478.6417 617.2783 714.8686
Frequencies -- 728.4973 786.2993 905.4232
Frequencies -- 1000.8521 1009.3523 1045.0559
Frequencies -- 1052.4088 1056.9474 1073.2713
Frequencies -- 1134.4290 1279.6998 1291.1061
Frequencies -- 1367.3684 1407.5916 1428.1451
Frequencies -- 1451.6054 1471.6484 1488.8877
Frequencies -- 1541.3926 1546.9739 1676.2008
Frequencies -- 1723.1635 2533.3470 3052.0352
Frequencies -- 3072.3139 3142.5181 3175.9221
Frequencies -- 3176.7554 3246.6418 3268.6392

anti-cis-MVK-oxide…FA

1	6	0	-1.204491	-0.289284	0.179447
2	8	0	-0.636027	-0.003481	1.281377
3	8	0	0.114207	1.173135	1.362642
4	8	0	1.132216	-1.243681	-0.736726
5	6	0	2.170139	-0.653559	-0.502650
6	8	0	2.330754	0.391270	0.275683
7	1	0	3.124247	-0.957045	-0.947481
8	1	0	1.453547	0.682670	0.711459
9	6	0	-1.864028	-1.622886	0.181619
10	6	0	-1.301847	0.547844	-0.990871
11	6	0	-0.919455	1.827305	-1.122501
12	1	0	-1.365943	-2.244171	-0.562172
13	1	0	-2.913278	-1.528862	-0.094753
14	1	0	-1.776075	-2.090435	1.156419
15	1	0	-1.783638	0.053676	-1.823398
16	1	0	-0.433607	2.350864	-0.319851
17	1	0	-1.116355	2.338842	-2.054295

Frequencies -- 39.8470 85.7734 91.7024
Frequencies -- 130.0329 140.2337 166.4205
Frequencies -- 233.1651 254.0281 308.4005
Frequencies -- 335.8177 350.7360 393.5006
Frequencies -- 415.9963 627.4836 709.1692
Frequencies -- 722.9086 807.4474 928.5132
Frequencies -- 1024.9488 1028.6116 1030.0566
Frequencies -- 1041.7744 1056.0029 1107.6739
Frequencies -- 1111.9206 1266.5495 1269.9390

Frequencies --	1350.0981	1407.6782	1411.3172
Frequencies --	1463.0391	1472.7066	1486.6933
Frequencies --	1519.7626	1553.1145	1661.2570
Frequencies --	1734.9712	2704.5444	3054.8259
Frequencies --	3065.4124	3132.2939	3174.3881
Frequencies --	3178.4393	3195.5629	3310.1617

HPBD…FA Intermdiate

syn-trans-HPBD…FA

1	6	0	-1.113347	0.483162	0.213380
2	6	0	-0.789321	0.219768	1.488724
3	6	0	-2.193604	-0.151394	-0.555793
4	6	0	-2.613372	-1.401824	-0.375908
5	8	0	-0.484608	1.381974	-0.596283
6	8	0	0.546691	2.099813	0.108319
7	1	0	0.646454	-1.043147	0.585778
8	1	0	-1.403495	-0.465438	2.048304
9	1	0	-0.011072	0.766084	1.991856
10	1	0	-2.634630	0.469306	-1.324331
11	1	0	-2.158531	-2.056579	0.353460
12	1	0	-3.425728	-1.802047	-0.962893
13	1	0	1.311624	1.519682	-0.092344
14	8	0	2.444316	0.160210	-0.423857
15	6	0	2.347215	-1.037303	-0.272221
16	8	0	1.334997	-1.682182	0.287448
17	1	0	3.118786	-1.740831	-0.593940

Frequencies --	46.5745	50.6495	76.8325
Frequencies --	101.0929	156.5767	166.8105
Frequencies --	191.9483	245.8305	252.7712
Frequencies --	358.4808	417.7017	516.8706
Frequencies --	590.4674	646.1497	674.9499
Frequencies --	751.6216	759.5421	797.7795
Frequencies --	861.0808	877.9018	930.4440
Frequencies --	970.8882	992.6994	1027.8803
Frequencies --	1076.1521	1089.2622	1200.4982
Frequencies --	1259.7690	1333.5512	1372.7183
Frequencies --	1420.5872	1430.2878	1471.8952
Frequencies --	1513.4595	1671.1401	1696.0523
Frequencies --	1769.4375	3094.2923	3169.3976
Frequencies --	3192.7316	3203.4099	3260.2551
Frequencies --	3303.4610	3391.3563	3517.8522

syn-cis-HPBD…FA

1	6	0	-1.106616	0.139014	0.525862
2	6	0	-0.549047	0.062319	1.747273
3	6	0	-2.115450	-0.806775	0.048019
4	6	0	-2.689988	-0.766416	-1.154468
5	8	0	-0.799963	1.062956	-0.423771
6	8	0	0.170524	2.012240	0.057824
7	1	0	0.983742	-0.980473	0.681893

8	1	0	-0.891338	-0.707007	2.420023
9	1	0	0.146686	0.802891	2.099755
10	1	0	-2.385068	-1.574248	0.760209
11	1	0	-2.436860	-0.006443	-1.877268
12	1	0	-3.432687	-1.498360	-1.432634
13	1	0	0.991865	1.571558	-0.248272
14	8	0	2.314600	0.447523	-0.697342
15	6	0	2.500861	-0.721527	-0.441810
16	8	0	1.744163	-1.492893	0.323271
17	1	0	3.350501	-1.286216	-0.832811

Frequencies --	39.4279	49.1022	87.3141
Frequencies --	117.3395	160.4916	169.4570
Frequencies --	190.3720	235.0266	253.7995
Frequencies --	367.4218	471.6775	489.3651
Frequencies --	583.9892	648.6302	675.2249
Frequencies --	753.7946	774.0511	796.6665
Frequencies --	854.5213	872.2213	933.9484
Frequencies --	971.2825	996.8084	1022.9112
Frequencies --	1073.6384	1076.7413	1199.9679
Frequencies --	1327.2299	1337.7576	1369.1387
Frequencies --	1415.2292	1429.8431	1466.5098
Frequencies --	1516.2999	1636.3173	1705.7378
Frequencies --	1769.6104	3095.2739	3178.1779
Frequencies --	3196.2712	3200.8333	3271.8125
Frequencies --	3302.4741	3411.2610	3512.8846

anti-trans-HPBD…FA

1	6	0	1.464908	-1.575683	-1.295623
2	6	0	1.707972	-0.384726	-0.750680
3	6	0	1.180891	0.032789	0.552291
4	6	0	0.988640	-0.769230	1.613557
5	8	0	-2.015175	0.831474	-0.492652
6	6	0	-2.469138	-0.259613	-0.234985
7	8	0	-1.858108	-1.232043	0.427411
8	8	0	0.933520	1.365220	0.736973
9	8	0	0.520379	1.973970	-0.514909
10	1	0	0.811225	-2.294492	-0.821601
11	1	0	1.906944	-1.855507	-2.239649
12	1	0	2.310763	0.346386	-1.268938
13	1	0	-0.955730	-0.948436	0.697641
14	1	0	1.352037	-1.783129	1.596644
15	1	0	0.584150	-0.369503	2.531077
16	1	0	-3.473313	-0.573346	-0.530749
17	1	0	-0.420645	1.707839	-0.526373

Frequencies --	41.0731	47.3932	94.9233
Frequencies --	127.0441	132.0509	172.8078
Frequencies --	175.5243	231.9939	269.1057
Frequencies --	318.6582	429.3863	524.8193
Frequencies --	574.5071	641.0168	662.1786
Frequencies --	737.6015	761.6599	822.5788
Frequencies --	832.9682	869.8769	913.3878

Frequencies --	969.1926	996.9055	1023.4182
Frequencies --	1076.1336	1091.9785	1190.4044
Frequencies --	1273.1133	1338.1650	1359.5755
Frequencies --	1418.3968	1428.0048	1471.9323
Frequencies --	1488.4244	1656.6350	1689.1365
Frequencies --	1774.2204	3091.9155	3165.6439
Frequencies --	3182.6729	3211.9066	3257.3763
Frequencies --	3284.2094	3432.1712	3569.8252

anti-cis-HPBD…FA

1	6	0	-1.053097	0.579828	0.464112
2	6	0	-0.475277	1.686648	0.963243
3	6	0	-1.953259	0.597989	-0.686000
4	6	0	-2.731588	-0.411313	-1.076458
5	8	0	-0.862414	-0.576964	1.179410
6	8	0	-0.485639	-1.662524	0.278729
7	1	0	-0.710618	2.656716	0.553938
8	1	0	1.242860	1.080634	-0.242961
9	1	0	0.147198	1.626993	1.842870
10	1	0	-1.987892	1.542785	-1.212807
11	1	0	-2.712735	-1.365982	-0.576934
12	1	0	-3.401260	-0.291060	-1.914662
13	1	0	0.485432	-1.552191	0.293355
14	8	0	2.227211	-1.067926	0.051458
15	6	0	2.719688	-0.095524	-0.472455
16	8	0	2.141515	1.087403	-0.636608
17	1	0	3.732841	-0.083565	-0.881366

Frequencies --	31.6378	35.8582	86.1594
Frequencies --	119.3072	135.7814	155.3607
Frequencies --	183.2784	218.9154	256.9134
Frequencies --	324.1310	419.4058	486.3974
Frequencies --	608.7873	634.7813	663.6092
Frequencies --	745.8742	764.5178	797.2146
Frequencies --	832.9567	886.4097	907.7395
Frequencies --	976.2320	987.8707	1022.8438
Frequencies --	1067.6367	1074.6317	1186.9295
Frequencies --	1328.7805	1335.9665	1357.7756
Frequencies --	1408.3983	1426.2500	1470.1134
Frequencies --	1484.9619	1632.0100	1702.8002
Frequencies --	1773.9460	3094.7773	3174.9689
Frequencies --	3178.2508	3188.6921	3275.6266
Frequencies --	3280.1709	3484.7147	3573.1287

OBD…OH…FA

1	6	0	1.508587	0.555215	-0.066165
2	6	0	2.214454	1.810886	-0.034072
3	6	0	2.243686	-0.731428	-0.018802
4	6	0	3.562627	-0.864269	0.110448
5	8	0	0.274484	0.558028	-0.137362
6	8	0	-0.758179	-1.645734	-0.075226
7	1	0	3.288084	1.879116	0.016630

8	1	0	1.627344	2.714077	-0.068161
9	1	0	1.597672	-1.595251	-0.092381
10	1	0	4.230740	-0.019711	0.192434
11	1	0	4.017632	-1.843097	0.142282
12	1	0	-1.230944	-1.158684	-0.783184
13	8	0	-2.799890	0.040203	-1.065746
14	6	0	-3.087446	0.444051	0.039852
15	8	0	-2.528648	0.064064	1.180526
16	1	0	-3.869483	1.186686	0.221336
17	1	0	-1.814631	-0.582354	0.965942

Frequencies --	12.8365	37.7491	41.6075
Frequencies --	64.7754	83.9403	89.2718
Frequencies --	129.2158	191.7825	203.1544
Frequencies --	221.7980	312.3144	331.9120
Frequencies --	444.5577	491.8802	539.2342
Frequencies --	556.5038	680.2494	701.6017
Frequencies --	732.4066	808.4855	828.7349
Frequencies --	878.3105	989.1015	995.1214
Frequencies --	1062.7285	1072.9715	1075.1237
Frequencies --	1217.4119	1319.9187	1323.9939
Frequencies --	1398.0611	1459.9535	1462.9129
Frequencies --	1490.7518	1629.4834	1732.0362
Frequencies --	1771.4272	3078.4852	3172.4788
Frequencies --	3190.6529	3206.5243	3257.8809
Frequencies --	3307.0517	3387.8060	3580.6863

HPBD-2…FA

1	6	0	-1.338124	-0.167992	0.235750
2	6	0	-2.132781	-0.160042	1.505226
3	6	0	-1.100700	0.884915	-0.514980
4	6	0	-0.992895	1.945669	-1.268136
5	8	0	-0.862444	-1.430957	-0.006455
6	8	0	-0.203241	-1.484491	-1.289077
7	1	0	-2.993170	-0.819877	1.401859
8	1	0	-2.475805	0.845804	1.725040
9	1	0	-1.527249	-0.523445	2.334869
10	1	0	0.707081	0.867400	0.555763
11	1	0	-1.719260	2.163303	-2.042128
12	1	0	-0.169583	2.642238	-1.162303
13	1	0	0.717482	-1.299076	-1.010083
14	8	0	2.270761	-0.729102	-0.273238
15	6	0	2.489139	0.204044	0.465404
16	8	0	1.598526	1.075388	0.919344
17	1	0	3.483847	0.437384	0.852811

Frequencies --	46.8022	51.4376	74.1932
Frequencies --	133.0190	149.9971	158.0070
Frequencies --	159.1250	191.4017	243.7461
Frequencies --	253.9419	289.6081	436.7437
Frequencies --	478.4352	629.6282	644.4804
Frequencies --	659.6410	672.7403	781.3356
Frequencies --	830.3892	926.4965	934.3199

Frequencies --	1016.0520	1041.6419	1073.3674
Frequencies --	1075.5051	1190.9225	1218.1425
Frequencies --	1334.5579	1364.4081	1417.4655
Frequencies --	1427.8560	1485.9345	1492.1258
Frequencies --	1511.4640	1523.6784	1770.4631
Frequencies --	2041.1642	3061.3768	3093.4485
Frequencies --	3123.1971	3124.5715	3168.1929
Frequencies --	3195.4936	3405.9078	3534.4605

Dioxole…FA

1	6	0	-2.736056	-1.111334	-0.716698
2	6	0	-1.731340	-0.128679	-0.237518
3	6	0	-1.252097	0.998767	-0.747768
4	6	0	-0.300557	1.594592	0.239170
5	8	0	-1.208145	-0.447460	0.991977
6	8	0	-0.112336	0.523859	1.202890
7	1	0	-3.553392	-1.197970	-0.001902
8	1	0	-3.136870	-0.789957	-1.673244
9	1	0	-2.284019	-2.095474	-0.829874
10	1	0	-1.526889	1.436101	-1.689435
11	1	0	-0.707061	2.468355	0.755816
12	1	0	0.687091	1.808274	-0.165842
13	1	0	1.242126	-0.547486	0.780361
14	8	0	1.956835	-1.169320	0.507202
15	6	0	2.714270	-0.580174	-0.412334
16	8	0	2.563341	0.534591	-0.851439
17	1	0	3.516124	-1.254229	-0.730027

Frequencies --	27.0442	32.2631	86.4180
Frequencies --	124.7751	157.0360	165.9333
Frequencies --	194.0732	240.7651	254.0830
Frequencies --	329.7220	555.3170	622.2615
Frequencies --	680.6148	722.0972	746.4992
Frequencies --	828.9997	912.7445	916.6697
Frequencies --	954.9729	1016.8334	1034.6405
Frequencies --	1066.2811	1076.0187	1079.9911
Frequencies --	1201.6205	1210.1360	1216.8408
Frequencies --	1290.7510	1379.5502	1388.1202
Frequencies --	1425.7684	1440.5033	1485.8000
Frequencies --	1502.6756	1526.9130	1743.0102
Frequencies --	1783.6200	3022.8944	3064.8210
Frequencies --	3067.2565	3114.1484	3126.3679
Frequencies --	3163.3924	3285.0520	3400.6808

Saddle Points

MVK-oxide *cis/trans* interconversion

syn-trans-MVK-oxide = *syn-cis*-MVK-oxide

1	6	0	2.327858	-0.267919	0.425627
2	6	0	1.381300	-0.133215	-0.497496
3	6	0	-0.027092	0.153355	-0.167281
4	6	0	-0.602629	1.490867	0.045170
5	8	0	-0.796694	-0.864200	-0.093452
6	8	0	-2.103652	-0.635657	0.189406
7	1	0	2.105556	-0.189953	1.480296
8	1	0	3.351766	-0.466552	0.146356
9	1	0	1.626162	-0.217122	-1.550508
10	1	0	-1.070284	1.516480	1.033036
11	1	0	-1.432790	1.629417	-0.652467
12	1	0	0.145734	2.268058	-0.060451

Frequencies --	-155.8236	160.3454	206.9403
Frequencies --	272.9053	318.6863	393.4493
Frequencies --	519.1815	618.1650	677.8188
Frequencies --	801.6223	973.9469	989.5462
Frequencies --	996.7350	1008.2812	1048.2105
Frequencies --	1090.0645	1299.6607	1324.2466
Frequencies --	1397.9023	1440.7421	1448.6849
Frequencies --	1456.7181	1494.5998	1693.0250
Frequencies --	3035.8504	3076.2762	3155.4400
Frequencies --	3168.9422	3179.8447	3258.5054

anti-trans-MVK-oxide = *anti-cis*-MVK-oxide

1	6	0	2.007829	-0.418699	-0.342971
2	6	0	0.984974	-0.461235	0.502459
3	6	0	-0.412755	-0.301218	0.080860
4	6	0	-1.331026	-1.454707	-0.099639
5	8	0	-0.925829	0.850993	-0.119854
6	8	0	-0.181649	1.963910	0.046691
7	1	0	1.863784	-0.218324	-1.394427
8	1	0	3.019565	-0.567451	0.002037
9	1	0	1.146198	-0.648731	1.558247
10	1	0	-2.328717	-1.110049	-0.356799
11	1	0	-1.377214	-2.045749	0.816530
12	1	0	-0.957925	-2.113760	-0.884538

Frequencies --	-172.4811	152.1270	208.0108
Frequencies --	231.6809	294.2586	330.2831
Frequencies --	521.8294	599.3025	696.2792
Frequencies --	802.6304	974.6524	982.0157
Frequencies --	993.4085	1013.3162	1031.6387
Frequencies --	1096.0715	1286.3799	1328.8923
Frequencies --	1414.9866	1434.1413	1473.1757
Frequencies --	1478.4513	1514.3980	1695.7927
Frequencies --	3046.9529	3100.6707	3156.9139
Frequencies --	3158.0516	3173.6061	3263.0241

MVK-oxide pre-reactive complex (PRC) *cis/trans* interconversion

syn-trans-MVK-oxide…FA = *syn-cis*-MVK-oxide…FA

1	6	0	-1.119161	-0.567213	0.048738
2	8	0	-0.340125	-0.999219	-0.847648
3	8	0	0.732073	-1.787407	-0.402364
4	8	0	0.949819	1.349499	0.510030
5	6	0	2.092030	1.138745	0.139620
6	8	0	2.566442	0.018246	-0.343349
7	1	0	2.867219	1.911785	0.180266
8	1	0	1.842763	-0.707639	-0.374539
9	6	0	-0.955142	-0.962295	1.456667
10	6	0	-2.210670	0.296792	-0.440682
11	6	0	-2.144870	1.621913	-0.367033
12	1	0	-1.845801	-0.725090	2.027776
13	1	0	-0.101418	-0.409203	1.851236
14	1	0	-0.692656	-2.018225	1.500223
15	1	0	-3.074078	-0.211703	-0.852441
16	1	0	-1.271235	2.114572	0.033441
17	1	0	-2.963582	2.228894	-0.723171

Frequencies --	-133.9452	58.2378	92.9406
Frequencies --	109.2354	123.4468	148.0852
Frequencies --	204.5360	247.3918	273.2048
Frequencies --	294.6929	339.5556	413.9882
Frequencies --	528.7150	607.7970	665.6096
Frequencies --	715.9043	798.3492	900.5086
Frequencies --	981.4570	1002.2993	1020.6978
Frequencies --	1046.3892	1053.4022	1105.8825
Frequencies --	1137.3757	1278.5620	1288.8692
Frequencies --	1325.8681	1380.8629	1411.1151
Frequencies --	1454.6381	1461.8802	1488.9666
Frequencies --	1512.6641	1543.5190	1687.4723
Frequencies --	1730.9835	2655.8785	3055.7842
Frequencies --	3062.5950	3125.5221	3167.5236
Frequencies --	3177.5878	3183.7870	3271.3087

anti-trans-MVK-oxide…FA = *anti-cis*-MVK-oxide…FA

1	6	0	-0.961063	0.388212	-0.330351
2	8	0	-0.359437	-0.199773	-1.269270
3	8	0	0.168229	-1.474750	-0.977504
4	8	0	1.312296	1.067136	0.746164
5	6	0	2.320541	0.396185	0.579893
6	8	0	2.415939	-0.738572	-0.056045
7	1	0	3.289796	0.715424	0.978062
8	1	0	1.498492	-1.051269	-0.435681
9	6	0	-1.401006	1.773659	-0.614996
10	6	0	-1.293572	-0.273518	0.942193
11	6	0	-2.376881	-1.030025	1.069193
12	1	0	-0.962181	2.422862	0.141944
13	1	0	-2.485010	1.838818	-0.524306
14	1	0	-1.078866	2.088497	-1.602519
15	1	0	-0.631902	-0.054704	1.766592

16	1	0	-3.026324	-1.246007	0.233210
17	1	0	-2.628348	-1.473023	2.020349

Frequencies --	-146.5178	54.4412	85.9999
Frequencies --	120.8789	154.5564	176.7642
Frequencies --	213.1547	245.6434	253.3806
Frequencies --	287.0740	331.8027	375.1406
Frequencies --	525.0896	599.9257	688.7097
Frequencies --	730.7215	793.4260	892.4437
Frequencies --	974.4115	1001.4054	1013.3538
Frequencies --	1036.1963	1058.9710	1103.9822
Frequencies --	1158.3710	1273.7360	1294.9430
Frequencies --	1320.1855	1405.7011	1410.4784
Frequencies --	1455.9622	1472.5534	1478.7020
Frequencies --	1553.3314	1579.7157	1691.1137
Frequencies --	1708.9486	2400.4030	3056.2864
Frequencies --	3063.3660	3131.2883	3171.3402
Frequencies --	3174.3852	3220.6571	3263.7551

MVK-oxide 1,4 H-atom transfer (TS1)

syn-trans-MVK-oxide = *syn-trans*-HPBD

1	6	0	2.457115	0.070170	0.032784
2	6	0	1.316473	-0.618112	-0.055817
3	6	0	0.010731	-0.001078	0.060352
4	6	0	-0.383451	1.346869	-0.052273
5	8	0	-0.977463	-0.869354	0.073675
6	8	0	-2.202077	-0.190060	-0.031532
7	1	0	2.460619	1.133723	0.220400
8	1	0	3.411786	-0.420028	-0.080885
9	1	0	1.320065	-1.687395	-0.219937
10	1	0	-1.560158	0.884857	-0.502121
11	1	0	-0.952622	1.745026	0.784583
12	1	0	0.351428	2.032029	-0.449460

Frequencies --	-1629.7695	122.2150	243.4351
Frequencies --	276.3347	470.4620	494.5344
Frequencies --	546.3726	635.4669	737.6518
Frequencies --	757.6567	904.9782	937.8313
Frequencies --	962.2955	990.4016	1027.7607
Frequencies --	1037.2315	1067.7425	1293.7400
Frequencies --	1346.8057	1351.3202	1466.9007
Frequencies --	1477.4722	1548.1219	1682.1434
Frequencies --	1839.3159	3110.2935	3174.6357
Frequencies --	3196.1290	3217.2816	3267.8889

syn-cis-MVK-oxide = *syn-cis*-HPBD

1	6	0	2.297324	-0.481816	0.019876
2	6	0	1.411571	0.515143	-0.053642
3	6	0	-0.026106	0.342616	0.063494
4	6	0	-1.022147	1.338205	0.014306
5	8	0	-0.472178	-0.889564	0.025294
6	8	0	-1.877499	-0.876092	-0.057740
7	1	0	1.982914	-1.505554	0.158002

8	1	0	3.356161	-0.285350	-0.047200
9	1	0	1.739610	1.538093	-0.170472
10	1	0	-1.833037	0.412863	-0.487093
11	1	0	-1.712231	1.363363	0.854875
12	1	0	-0.699849	2.316944	-0.312739

Frequencies -- -1621.2741 81.9648 229.5546
Frequencies -- 266.0867 476.5977 496.4703
Frequencies -- 537.9626 646.5707 725.1641
Frequencies -- 751.7414 903.9521 944.4949
Frequencies -- 956.8335 989.7721 1025.4711
Frequencies -- 1033.7173 1086.5539 1315.6873
Frequencies -- 1347.7589 1368.0379 1436.4872
Frequencies -- 1488.4045 1534.2193 1686.2915
Frequencies -- 1843.8806 3107.0926 3177.1727
Frequencies -- 3204.9130 3211.2610 3271.6925

MVK-oxide + HC(O)OH Spectator Catalysis (TS_{spec})

syn-trans-MVK-oxide…FA = *syn-trans*-HPBD…FA

1	6	0	-1.328526	-0.194698	0.112768
2	8	0	-0.658231	-1.292444	-0.201755
3	8	0	0.449685	-1.418902	0.681626
4	8	0	2.182037	1.458940	0.139373
5	6	0	2.899587	0.670069	-0.434077
6	8	0	2.691533	-0.629139	-0.568687
7	1	0	3.835239	0.961004	-0.923377
8	1	0	1.846107	-0.889006	-0.111422
9	6	0	-0.778502	0.591520	1.127904
10	6	0	-2.625720	-0.130048	-0.534413
11	6	0	-3.386817	0.965897	-0.505154
12	1	0	-1.453940	1.249714	1.652974
13	1	0	0.212579	1.006974	0.936098
14	1	0	-0.083482	-0.519388	1.484621
15	1	0	-2.944342	-1.022733	-1.055143
16	1	0	-3.056953	1.867085	-0.009732
17	1	0	-4.355519	0.982263	-0.980646

Frequencies -- -1619.5992 36.1864 41.4330
Frequencies -- 86.0767 127.5592 134.9963
Frequencies -- 203.5753 209.0236 251.3755
Frequencies -- 312.8601 474.3481 495.0176
Frequencies -- 586.0329 636.1406 685.9332
Frequencies -- 750.5329 778.9893 910.2849
Frequencies -- 933.6084 957.7666 1004.7380
Frequencies -- 1008.0108 1027.0935 1039.9439
Frequencies -- 1072.1405 1094.7722 1221.8891
Frequencies -- 1281.0016 1312.4225 1353.3064
Frequencies -- 1395.2671 1436.5805 1467.6309
Frequencies -- 1471.5440 1566.7206 1684.0863
Frequencies -- 1769.5521 1809.4227 3056.2536
Frequencies -- 3058.8757 3175.4253 3199.9618
Frequencies -- 3209.2346 3226.7428 3269.5534

syn-cis-MVK-oxide…FA = *syn-cis*-HPBD…FA

1	6	0	1.310000	-0.362991	0.185501
2	8	0	0.883397	0.875936	0.346937
3	8	0	-0.257914	0.855669	1.201332
4	8	0	-2.449001	-1.155439	-0.431711
5	6	0	-2.947866	-0.074322	-0.653856
6	8	0	-2.481681	1.101419	-0.269139
7	1	0	-3.876288	0.047718	-1.221901
8	1	0	-1.644493	0.982018	0.259086
9	6	0	0.531967	-1.363316	0.771960
10	6	0	2.626054	-0.500574	-0.417190
11	6	0	3.337675	0.522186	-0.897563
12	1	0	1.021494	-2.309697	0.948628
13	1	0	-0.503434	-1.444341	0.432118
14	1	0	0.035970	-0.400945	1.566146
15	1	0	2.990983	-1.514634	-0.489364
16	1	0	2.973949	1.537346	-0.843203
17	1	0	4.296433	0.355963	-1.363977

Frequencies --	-1614.8640	32.0659	42.9546
Frequencies --	79.6974	104.0764	138.5301
Frequencies --	194.3823	206.0776	247.0365
Frequencies --	312.6558	476.4856	502.0277
Frequencies --	578.6757	643.1789	687.4903
Frequencies --	738.4168	775.3117	907.2298
Frequencies --	936.2919	959.0045	1003.8376
Frequencies --	1015.3897	1026.4607	1037.6955
Frequencies --	1082.8387	1098.6969	1224.4337
Frequencies --	1296.4780	1327.2110	1366.0240
Frequencies --	1397.4520	1434.8454	1442.8708
Frequencies --	1483.5084	1551.3566	1687.7454
Frequencies --	1767.3053	1813.7509	3042.2522
Frequencies --	3056.9034	3178.4842	3183.5276
Frequencies --	3211.1108	3219.7403	3273.2819

MVK-oxide + HC(O)OH Chemical catalysis (TS2)

syn-trans-MVK-oxide…FA = *syn-trans*-HPBD…FA

1	6	0	-1.080704	0.377209	0.188540
2	6	0	-0.555295	-0.356308	1.279037
3	6	0	-2.239660	0.027415	-0.620712
4	6	0	-3.035280	-1.011786	-0.361340
5	8	0	-0.489331	1.425459	-0.300170
6	8	0	0.673982	1.830693	0.436289
7	1	0	0.371272	-0.947087	0.762110
8	1	0	-1.238463	-1.081474	1.698825
9	1	0	-0.051844	0.267701	2.007860
10	1	0	-2.418070	0.667711	-1.472752
11	1	0	-2.872813	-1.666940	0.480550
12	1	0	-3.873946	-1.232751	-1.003573
13	1	0	1.406116	1.164991	0.009601
14	8	0	2.356160	0.334044	-0.562840

15	6	0	2.384541	-0.914667	-0.403353
16	8	0	1.530251	-1.649541	0.156394
17	1	0	3.267642	-1.428570	-0.813027

Frequencies --	-534.8581	49.5601	61.5051
Frequencies --	93.0114	133.7931	197.7074
Frequencies --	255.7488	269.8051	376.9820
Frequencies --	419.6663	482.3724	487.0736
Frequencies --	549.5547	602.6145	715.7893
Frequencies --	762.5884	855.8855	889.6618
Frequencies --	937.3861	1015.0995	1028.4686
Frequencies --	1034.6164	1036.7626	1076.1186
Frequencies --	1094.2163	1172.0474	1317.9591
Frequencies --	1359.0010	1370.9333	1376.8074
Frequencies --	1413.0707	1443.5561	1474.8938
Frequencies --	1493.0554	1591.1083	1667.1251
Frequencies --	1687.4280	1773.2908	1995.0004
Frequencies --	2986.7198	3141.5776	3183.5139
Frequencies --	3210.4235	3229.1369	3275.6609

syn-cis-MVK-oxide…FA = *syn-cis*-HPBD…FA

1	6	0	-1.078834	-0.103432	0.481965
2	6	0	-0.270354	-0.805076	1.416639
3	6	0	-2.222285	-0.718156	-0.182706
4	6	0	-2.940371	-0.111522	-1.131420
5	8	0	-0.801093	1.088736	0.070501
6	8	0	0.339628	1.673008	0.721539
7	1	0	0.669001	-1.105688	0.740330
8	1	0	-0.740205	-1.702353	1.798546
9	1	0	0.180093	-0.165547	2.166731
10	1	0	-2.460005	-1.718666	0.144950
11	1	0	-2.703708	0.886861	-1.467265
12	1	0	-3.781495	-0.610554	-1.587586
13	1	0	1.145067	1.250511	0.106381
14	8	0	2.138429	0.772783	-0.669324
15	6	0	2.468582	-0.446855	-0.682376
16	8	0	1.895156	-1.414935	-0.129125
17	1	0	3.373860	-0.681050	-1.263425

Frequencies --	-489.0263	32.9454	58.7812
Frequencies --	102.2931	126.4769	198.1492
Frequencies --	234.9037	259.1731	368.9102
Frequencies --	418.9812	477.1252	484.1433
Frequencies --	553.6979	606.3183	694.0498
Frequencies --	756.6221	844.5250	908.9340
Frequencies --	938.7210	1021.9035	1030.1369
Frequencies --	1037.3734	1062.5528	1076.2332
Frequencies --	1103.6397	1221.9108	1319.3426
Frequencies --	1353.8798	1366.0180	1378.6005
Frequencies --	1413.3946	1442.8830	1462.8745
Frequencies --	1497.8126	1561.1631	1668.2735
Frequencies --	1684.2685	1829.9010	1883.8613
Frequencies --	2985.5777	3133.1881	3180.8731

Frequencies -- 3218.7206 3223.8573 3277.1215

anti-trans-MVK-oxide…FA = *anti-trans*-HPBD…FA

1	6	0	-0.640244	1.802366	-1.339619
2	6	0	-1.220185	0.682845	-0.896293
3	6	0	-1.048998	0.233095	0.466616
4	6	0	-0.556621	1.048560	1.527261
5	8	0	1.326398	-1.152261	-0.575219
6	6	0	2.165620	-0.298990	-0.191075
7	8	0	1.987142	0.708599	0.544640
8	8	0	-1.212686	-1.017049	0.781594
9	8	0	-1.083955	-1.892479	-0.361489
10	1	0	0.020100	2.387982	-0.718116
11	1	0	-0.773879	2.119491	-2.362551
12	1	0	-1.792417	0.041082	-1.545933
13	1	0	0.586439	0.946324	1.179359
14	1	0	-0.853372	2.087734	1.490449
15	1	0	-0.630426	0.591112	2.506699
16	1	0	3.198293	-0.444917	-0.551409
17	1	0	-0.087352	-1.710544	-0.516051

Frequencies -- -429.6501 59.6039 82.6856
Frequencies -- 96.7238 121.6146 163.8226
Frequencies -- 238.5437 287.1099 329.8363
Frequencies -- 361.0465 430.5272 501.9798
Frequencies -- 541.4288 575.7868 705.0996
Frequencies -- 750.6971 806.7752 870.4764
Frequencies -- 918.4146 948.6564 1011.1905
Frequencies -- 1025.9536 1046.2794 1075.4536
Frequencies -- 1079.5032 1180.8126 1313.9823
Frequencies -- 1371.2961 1409.5689 1418.6823
Frequencies -- 1424.9234 1436.8928 1478.7021
Frequencies -- 1509.5474 1556.4926 1630.1030
Frequencies -- 1673.9240 1886.9935 2766.8441
Frequencies -- 2954.7679 3143.0130 3181.5497
Frequencies -- 3228.9677 3241.7875 3276.9028

anti-cis-MVK-oxide…FA = *anti-cis*-HPBD…FA

1	6	0	0.598672	0.737540	-0.332058
2	6	0	-0.295281	1.822561	-0.578511
3	6	0	1.219267	0.577712	0.968460
4	6	0	2.384499	-0.035089	1.190521
5	8	0	0.766688	-0.055524	-1.353358
6	8	0	1.130270	-1.408256	-0.985489
7	1	0	-0.095475	2.709318	0.010972
8	1	0	-1.280780	1.300814	-0.145245
9	1	0	-0.491549	2.010575	-1.627718
10	1	0	0.713363	1.110848	1.759309
11	1	0	2.909323	-0.564347	0.412814
12	1	0	2.831226	-0.000616	2.172668
13	1	0	0.307239	-1.601387	-0.438804
14	8	0	-0.953972	-1.174206	0.473205

15	6	0	-2.143702	-0.751914	0.411857
16	8	0	-2.509145	0.442599	0.291535
17	1	0	-2.944811	-1.506958	0.487248

Frequencies --	-368.1729	52.5610	82.4123
Frequencies --	111.9447	127.8068	154.7988
Frequencies --	249.6457	267.9650	300.1926
Frequencies --	353.3522	396.9342	482.8032
Frequencies --	538.0406	616.3751	709.0883
Frequencies --	746.9811	809.5570	828.4949
Frequencies --	907.2965	917.4848	1015.4159
Frequencies --	1018.4944	1051.8117	1077.9866
Frequencies --	1098.8167	1164.9608	1340.3861
Frequencies --	1369.9285	1399.6753	1410.3061
Frequencies --	1411.4989	1427.5623	1472.4686
Frequencies --	1505.4355	1535.9277	1582.9696
Frequencies --	1681.3705	1873.6266	2952.2355
Frequencies --	3063.5428	3130.7084	3186.6097
Frequencies --	3215.0857	3219.0675	3288.4898

MVK-oxide + HC(O)OH 1,4-insertion (TS3)

syn-trans-MVK-oxide…FA = *syn-trans*-HPBF Adduct

1	6	0	0.735502	0.454862	0.005429
2	8	0	-0.012061	1.158611	-0.764566
3	8	0	-1.165269	1.718647	-0.142895
4	8	0	-0.488945	-1.447803	0.047960
5	6	0	-1.725710	-1.379711	-0.017457
6	8	0	-2.456497	-0.330435	-0.094877
7	1	0	-2.299636	-2.314001	-0.008477
8	1	0	-1.862852	0.675446	-0.120004
9	6	0	0.665065	0.556642	1.481842
10	6	0	1.860444	-0.120030	-0.717072
11	6	0	2.908772	-0.687222	-0.120910
12	1	0	1.082850	-0.330317	1.941562
13	1	0	1.249719	1.432001	1.776493
14	1	0	-0.355806	0.708391	1.801768
15	1	0	1.796939	-0.048340	-1.793121
16	1	0	2.983701	-0.776058	0.951796
17	1	0	3.722827	-1.086513	-0.705978

Frequencies --	-598.0338	58.5295	83.8810
Frequencies --	142.1704	169.6873	192.1403
Frequencies --	250.3268	271.1921	305.4575
Frequencies --	345.1720	376.8882	461.5846
Frequencies --	484.5414	575.6331	662.7502
Frequencies --	706.2328	774.5847	819.0039
Frequencies --	939.2021	995.0411	1000.5989
Frequencies --	1028.5869	1060.3462	1066.7508
Frequencies --	1078.1853	1271.7963	1318.4128
Frequencies --	1346.0554	1354.1718	1403.3264
Frequencies --	1417.4923	1456.9270	1475.3778
Frequencies --	1496.8015	1526.9577	1669.0611

Frequencies --	1691.6501		1744.9004		3039.1798
Frequencies --	3057.8435		3169.0449		3183.6576
Frequencies --	3213.6016		3225.2961		3273.7312

syn-cis-MVK-oxide…FA = *syn-trans*-HPBF Adduct

1	6	0	0.765938	0.251319	0.369668
2	8	0	0.401376	0.949070	-0.634030
3	8	0	-0.730201	1.788150	-0.400938
4	8	0	-0.765726	-1.435154	0.230274
5	6	0	-1.898953	-1.162037	-0.182719
6	8	0	-2.363178	-0.015020	-0.533569
7	1	0	-2.635756	-1.968065	-0.274764
8	1	0	-1.627624	0.845160	-0.478002
9	6	0	0.320028	0.552866	1.749948
10	6	0	1.906477	-0.630983	0.129397
11	6	0	2.738632	-0.487794	-0.901713
12	1	0	0.514166	-0.296839	2.394435
13	1	0	0.911469	1.407665	2.091403
14	1	0	-0.722029	0.838039	1.777438
15	1	0	2.049293	-1.404518	0.867968
16	1	0	2.600420	0.294747	-1.632516
17	1	0	3.579156	-1.152767	-1.027342

Frequencies --	-335.6255	52.6315	81.0603
Frequencies --	135.1120	181.6510	183.0212
Frequencies --	229.4599	266.1835	316.4766
Frequencies --	346.8078	381.7988	435.7899
Frequencies --	503.2674	604.7698	676.1709
Frequencies --	750.3469	784.6604	892.3250
Frequencies --	984.6236	1008.8152	1015.6960
Frequencies --	1025.9930	1064.8159	1065.5608
Frequencies --	1111.3095	1261.9815	1288.8785
Frequencies --	1340.9716	1342.1872	1411.9670
Frequencies --	1417.0960	1451.9362	1474.0738
Frequencies --	1493.0829	1542.4368	1656.9518
Frequencies --	1690.2947	1758.4095	3046.9518
Frequencies --	3049.7852	3157.4781	3179.0293
Frequencies --	3220.3575	3225.5885	3274.1898

anti-trans-MVK-oxide…FA = *anti-trans*-HPBF Adduct

1	6	0	0.825182	0.427532	0.292669
2	6	0	1.630233	0.108083	1.501824
3	6	0	1.143999	-0.063969	-1.035023
4	6	0	2.126701	-0.940390	-1.251695
5	8	0	0.020819	1.410634	0.466041
6	8	0	-0.834550	1.703592	-0.639281
7	1	0	2.631771	0.523829	1.394623
8	1	0	1.699350	-0.968701	1.616014
9	1	0	1.152771	0.532449	2.378350
10	1	0	0.560690	0.356526	-1.836691
11	1	0	2.701869	-1.377157	-0.449135
12	1	0	2.370537	-1.252472	-2.255728

13	1	0	-1.633065	0.739262	-0.512437
14	8	0	-2.340300	-0.177030	-0.379581
15	6	0	-1.813030	-1.171180	0.232822
16	8	0	-0.653590	-1.274934	0.658286
17	1	0	-2.501468	-2.012293	0.377709

Frequencies --	-533.3679	48.5684	85.3667
Frequencies --	132.3468	173.0964	195.0681
Frequencies --	251.9218	273.6320	298.8173
Frequencies --	336.1784	352.4457	441.5295
Frequencies --	475.0791	601.3365	644.9041
Frequencies --	738.5756	774.3844	805.1464
Frequencies --	927.4014	1004.9935	1007.3295
Frequencies --	1046.1509	1062.5612	1066.6956
Frequencies --	1076.7233	1264.7986	1302.0853
Frequencies --	1351.9233	1362.2992	1403.0938
Frequencies --	1430.0085	1442.7723	1465.7720
Frequencies --	1493.2001	1542.5711	1673.9648
Frequencies --	1683.2205	1747.2926	3038.7694
Frequencies --	3075.3584	3157.2057	3178.5405
Frequencies --	3188.7304	3250.1203	3270.7228

anti-cis-MVK-oxide…FA = *anti-cis*-HPBF Adduct

1	6	0	0.972909	-0.331584	0.199133
2	6	0	1.683363	-1.637282	0.302893
3	6	0	1.149660	0.459347	-1.009931
4	6	0	1.065260	1.788171	-1.126332
5	8	0	0.516510	0.072723	1.323896
6	8	0	-0.248626	1.277296	1.303086
7	1	0	2.757821	-1.453059	0.344982
8	1	0	1.464274	-2.231934	-0.578185
9	1	0	1.369900	-2.168903	1.194666
10	1	0	1.454483	-0.137129	-1.857603
11	1	0	0.754268	2.408816	-0.304950
12	1	0	1.323470	2.251161	-2.067801
13	1	0	-1.269163	0.835194	0.692960
14	8	0	-2.182971	0.408244	0.125782
15	6	0	-1.963032	-0.665550	-0.537013
16	8	0	-0.890845	-1.272944	-0.673539
17	1	0	-2.856550	-1.065310	-1.030362

Frequencies --	-510.7037	54.2275	109.8598
Frequencies --	145.6613	177.3272	196.6995
Frequencies --	256.2488	298.1436	312.5872
Frequencies --	330.0583	356.7362	397.6463
Frequencies --	472.3527	618.9639	646.0874
Frequencies --	750.4431	782.8750	817.8670
Frequencies --	935.0425	1025.8260	1035.7259
Frequencies --	1039.1614	1062.1600	1065.5649
Frequencies --	1109.5076	1244.6272	1267.9168
Frequencies --	1351.0535	1352.6226	1404.8237
Frequencies --	1414.2389	1458.4383	1468.2622
Frequencies --	1491.2436	1558.0727	1670.3953

Frequencies --	1675.7153	1749.5880	3043.5184
Frequencies --	3066.4061	3150.4026	3179.3026
Frequencies --	3189.7453	3206.8386	3300.4674

MVK-oxide + HC(O)OH Chemical Catalysis (Vinyl H-atom)

anti-trans-MVK-oxide…FA = *trans*-HPBD-2

1	6	0	-1.319153	-0.276721	0.173401
2	6	0	-2.387923	-0.368121	1.204644
3	6	0	-0.759708	0.929188	-0.247433
4	6	0	-1.276074	1.962763	-0.905043
5	8	0	-0.836120	-1.436892	-0.150040
6	8	0	0.108672	-1.348954	-1.239277
7	1	0	-3.278063	0.130055	0.818655
8	1	0	-2.076706	0.172259	2.096377
9	1	0	-2.610187	-1.401338	1.452813
10	1	0	0.459623	1.027897	0.137577
11	1	0	-2.239337	1.922265	-1.398843
12	1	0	-0.702639	2.871098	-1.023748
13	1	0	0.982382	-1.172520	-0.706832
14	8	0	2.211878	-0.878693	0.060934
15	6	0	2.479167	0.268026	0.471258
16	8	0	1.709064	1.278337	0.528751
17	1	0	3.499114	0.449090	0.840103

Frequencies --	-896.7737	56.7959	74.2582
Frequencies --	103.1404	121.3808	155.2350
Frequencies --	208.2114	221.7051	249.0315
Frequencies --	301.8563	383.9833	448.2472
Frequencies --	494.7112	595.5098	638.7857
Frequencies --	744.2849	766.0403	838.9508
Frequencies --	926.7701	982.4224	1035.4183
Frequencies --	1039.1149	1049.1226	1073.7053
Frequencies --	1102.2736	1212.9510	1307.9068
Frequencies --	1362.1666	1395.4673	1413.7908
Frequencies --	1418.8840	1466.0078	1479.8649
Frequencies --	1488.3922	1542.5313	1640.0440
Frequencies --	1679.1691	1761.6799	2501.1101
Frequencies --	3002.5854	3062.5602	3132.5949
Frequencies --	3139.3827	3173.4830	3230.7535

HPBD Product Acid Catalysis ($TS_{H,exchange}$)

syn-trans-HPBD…FA = *syn-trans*-HPBD…FA

1	6	0	-1.531737	0.270165	-0.142604
2	6	0	-1.792370	1.574484	-0.068199
3	6	0	-2.513318	-0.819516	-0.216003
4	6	0	-3.702038	-0.799923	0.383668
5	8	0	-0.275133	-0.296688	-0.186703
6	8	0	0.745086	0.731020	-0.211635
7	1	0	-2.819474	1.896627	-0.090742
8	1	0	-1.008943	2.308147	-0.010953
9	1	0	-2.211226	-1.681185	-0.797475
10	1	0	-4.007590	0.028866	1.005610
11	1	0	-4.396354	-1.617547	0.263482
12	1	0	1.485349	0.423226	0.724233
13	8	0	2.502918	-0.024331	1.209172
14	6	0	3.140356	-0.437784	0.194828
15	8	0	2.727388	-0.331458	-0.998447
16	1	0	4.105615	-0.914081	0.359495
17	1	0	1.645198	0.203053	-0.862887

Frequencies --	-1603.1048	1.4786	57.2097
Frequencies --	67.7031	99.9953	207.1727
Frequencies --	224.2705	287.8611	329.1158
Frequencies --	395.8273	470.6643	571.9532
Frequencies --	576.5467	643.6319	733.7901
Frequencies --	744.2329	850.2178	856.1461
Frequencies --	866.7927	922.2949	965.4762
Frequencies --	994.5418	1026.5167	1080.6693
Frequencies --	1088.8540	1197.5386	1292.2541
Frequencies --	1332.9295	1374.5493	1377.2372
Frequencies --	1388.5928	1426.6051	1469.2157
Frequencies --	1532.8067	1597.8087	1693.6358
Frequencies --	1706.5763	1712.4758	1933.7363
Frequencies --	3138.3969	3168.4695	3183.9081
Frequencies --	3209.9838	3260.2795	3309.7109

syn-cis-HPBD…FA = *syn-cis*-HPBD…FA

1	6	0	1.657435	0.503052	-0.000045
2	6	0	1.846634	1.824970	0.000007
3	6	0	2.743622	-0.472651	0.000191
4	6	0	2.597969	-1.798524	0.000151
5	8	0	0.435853	-0.127004	-0.000327
6	8	0	-0.634645	0.846972	-0.000517
7	1	0	2.857898	2.196212	0.000241
8	1	0	1.029099	2.522296	-0.000180
9	1	0	3.731329	-0.032559	0.000412
10	1	0	1.624726	-2.264208	-0.000068
11	1	0	3.461951	-2.445140	0.000338
12	1	0	-1.440069	0.374101	-0.806993
13	8	0	-2.467883	-0.184351	-1.119935
14	6	0	-2.982703	-0.477802	0.000313
15	8	0	-2.467573	-0.183501	1.120196

16	1	0	-3.928842	-1.016598	0.000650
17	1	0	-1.439846	0.374710	0.806548

Frequencies --	-1600.7447	-7.0920	55.2583
Frequencies --	57.8931	142.4909	208.3735
Frequencies --	224.1359	270.3055	338.6807
Frequencies --	451.1011	472.7713	534.9090
Frequencies --	572.8371	655.7153	727.1813
Frequencies --	764.1784	851.8203	855.2240
Frequencies --	858.5466	928.0467	951.1098
Frequencies --	1000.0804	1021.8736	1068.5207
Frequencies --	1080.8562	1231.4735	1325.4597
Frequencies --	1347.9790	1374.6261	1377.2054
Frequencies --	1389.6664	1422.5595	1468.5169
Frequencies --	1532.9088	1599.5590	1654.6886
Frequencies --	1711.8075	1720.6024	1931.6378
Frequencies --	3139.8580	3177.5529	3195.9745
Frequencies --	3207.6910	3269.0680	3310.4980

anti-trans-HPBD…FA = *anti-trans*-HPBD…FA

1	6	0	-1.515069	0.486711	-0.299936
2	6	0	-2.029065	1.707796	-0.135021
3	6	0	-2.225960	-0.789149	-0.201391
4	6	0	-3.234437	-1.012709	0.639356
5	8	0	-0.206074	0.429831	-0.734773
6	8	0	0.482173	-0.626068	0.025280
7	1	0	-3.090650	1.836126	-0.002841
8	1	0	-1.395566	2.578520	-0.190875
9	1	0	-1.877349	-1.573221	-0.859897
10	1	0	-3.556729	-0.259565	1.344276
11	1	0	-3.754054	-1.958656	0.647781
12	1	0	1.512763	-0.759346	-0.597901
13	8	0	2.726217	-0.622702	-0.778824
14	6	0	3.079296	0.068513	0.222242
15	8	0	2.294698	0.445861	1.143075
16	1	0	4.127362	0.356825	0.297668
17	1	0	1.209525	-0.003030	0.772228

Frequencies --	-1600.6277	17.9084	53.5243
Frequencies --	81.5663	115.3588	173.4415
Frequencies --	228.3193	284.8755	328.9778
Frequencies --	433.2394	457.3290	558.5721
Frequencies --	568.9826	625.4588	737.7972
Frequencies --	761.4659	824.3384	850.3551
Frequencies --	884.2050	902.6315	964.6721
Frequencies --	976.7683	1025.0063	1079.8868
Frequencies --	1091.4430	1180.0407	1284.4578
Frequencies --	1337.2008	1374.7083	1378.3778
Frequencies --	1386.8911	1421.8023	1469.4305
Frequencies --	1536.0214	1582.9452	1684.3362
Frequencies --	1691.4294	1716.4142	1946.5765
Frequencies --	3128.5364	3166.9029	3190.0080
Frequencies --	3193.4707	3258.4562	3288.4564

anti-cis-HPBD…FA = *anti-cis*-HPBD…FA

1	6	0	1.560820	0.628946	0.179133
2	6	0	1.713670	1.955560	0.222311
3	6	0	2.579042	-0.313708	-0.268411
4	6	0	2.490189	-1.639485	-0.163847
5	8	0	0.385456	0.125355	0.710986
6	8	0	-0.350010	-0.546421	-0.382983
7	1	0	2.654467	2.406915	-0.051689
8	1	0	0.909900	2.587630	0.564192
9	1	0	3.461878	0.139327	-0.700309
10	1	0	1.617206	-2.113164	0.256655
11	1	0	3.293810	-2.275114	-0.502762
12	1	0	-1.304479	-0.977166	0.204860
13	8	0	-2.503835	-0.982253	0.546174
14	6	0	-2.951162	0.063174	-0.010574
15	8	0	-2.262294	0.834170	-0.743976
16	1	0	-3.998964	0.317221	0.149651
17	1	0	-1.143705	0.300622	-0.713884

Frequencies --	-1590.0275	17.9402	51.3294
Frequencies --	90.3258	147.7162	148.6563
Frequencies --	213.4848	293.4471	327.9973
Frequencies --	423.7610	464.5927	569.1739
Frequencies --	575.0792	630.1288	742.8803
Frequencies --	765.5214	833.6329	839.6901
Frequencies --	877.8500	923.4904	960.7476
Frequencies --	974.0755	1023.7322	1057.1576
Frequencies --	1079.6612	1211.0372	1325.6118
Frequencies --	1327.6159	1375.0725	1379.9716
Frequencies --	1391.8436	1412.3241	1469.6310
Frequencies --	1543.9967	1572.7716	1649.7743
Frequencies --	1711.6395	1717.7210	1953.5116
Frequencies --	3123.3689	3176.8209	3184.2182
Frequencies --	3189.1887	3273.2006	3283.1271

MVK-oxide + HC(O)OH SOZ Formation (TS_{SOZ})

syn-trans-MVK-oxide…FA = SOZ

1	6	0	-0.784362	0.304551	0.221130
2	8	0	-0.120481	1.397401	-0.018725
3	8	0	1.214481	1.291813	0.362159
4	6	0	1.693912	-0.220558	-0.699116
5	8	0	0.584511	-0.763544	-0.932682
6	8	0	2.607222	-0.815652	0.115525
7	1	0	2.198051	0.405698	-1.429815
8	1	0	2.143842	-1.530395	0.568941
9	6	0	-0.561550	-0.494008	1.459371
10	6	0	-2.037806	0.262804	-0.516733
11	6	0	-2.997793	-0.634292	-0.288979
12	1	0	-1.311294	-0.192946	2.194217
13	1	0	-0.677580	-1.553133	1.257517
14	1	0	0.427048	-0.290476	1.850267

15	1	0	-2.133094	0.998978	-1.301931
16	1	0	-2.906734	-1.389698	0.476822
17	1	0	-3.900503	-0.639156	-0.880263

Frequencies --	-360.3426	83.3302	91.9426
Frequencies --	161.9644	220.1409	252.0331
Frequencies --	264.5245	308.8371	348.3251
Frequencies --	396.4673	421.1496	491.0744
Frequencies --	505.9320	593.9885	613.0639
Frequencies --	654.8811	698.2384	805.6680
Frequencies --	958.7928	983.7118	993.1586
Frequencies --	1028.9134	1041.1489	1067.4147
Frequencies --	1075.2862	1122.0594	1297.7853
Frequencies --	1308.8522	1344.2672	1367.0865
Frequencies --	1398.6596	1439.6015	1464.3650
Frequencies --	1504.8121	1513.0169	1547.6288
Frequencies --	1688.1198	3057.3002	3133.0402
Frequencies --	3151.8502	3179.4857	3203.9918
Frequencies --	3210.3938	3269.2902	3794.3344

syn-trans-MVK-oxide…FA = SOZ Geometry 2

1	6	0	-0.795699	0.326159	-0.210104
2	8	0	0.088732	0.500830	-1.147136
3	8	0	1.230002	1.153056	-0.678518
4	6	0	1.733543	-0.199624	0.596996
5	8	0	0.617903	-0.651784	0.961780
6	8	0	2.590214	-0.987978	-0.096953
7	1	0	2.281353	0.549407	1.162984
8	1	0	2.069435	-1.737720	-0.412420
9	6	0	-1.056104	1.354912	0.833071
10	6	0	-1.789223	-0.667997	-0.590588
11	6	0	-2.905537	-0.896982	0.101906
12	1	0	-1.902289	1.962039	0.503956
13	1	0	-1.304353	0.882764	1.776844
14	1	0	-0.182002	1.980388	0.953257
15	1	0	-1.549561	-1.244465	-1.472910
16	1	0	-3.148234	-0.342677	0.995734
17	1	0	-3.601039	-1.661532	-0.208514

Frequencies --	-375.3655	62.6853	93.6043
Frequencies --	178.5469	202.4328	215.6575
Frequencies --	263.1857	287.4049	359.7552
Frequencies --	388.9185	435.7127	489.4479
Frequencies --	506.9477	593.3510	630.0092
Frequencies --	683.5802	706.8002	804.3914
Frequencies --	952.2295	981.8290	994.0522
Frequencies --	1029.0509	1043.9073	1072.0856
Frequencies --	1074.6048	1138.8653	1305.8611
Frequencies --	1310.8909	1339.1331	1357.1059
Frequencies --	1399.1749	1442.4413	1462.3623
Frequencies --	1501.6016	1504.1030	1548.0373
Frequencies --	1688.0862	3058.0552	3126.2501
Frequencies --	3158.9405	3179.9044	3206.0361

Frequencies -- 3212.5352 3270.1096 3783.3239

HPBD…FA = OBD…OH…FA; *syn-trans*

1	6	0	1.719273	-0.210677	-0.176920
2	6	0	2.994206	-0.100560	0.358866
3	6	0	0.893136	0.946747	-0.567019
4	6	0	1.009504	2.153778	-0.022497
5	8	0	1.301979	-1.393095	-0.428190
6	8	0	-0.295986	-1.668250	0.439796
7	1	0	3.546495	0.824790	0.317136
8	1	0	3.479351	-0.993947	0.717468
9	1	0	0.131489	0.738166	-1.305989
10	1	0	1.732290	2.360878	0.754366
11	1	0	0.366833	2.966894	-0.324012
12	1	0	-0.787000	-1.716714	-0.397072
13	8	0	-2.453863	-0.232725	-0.991976
14	6	0	-2.676586	0.378354	0.030080
15	8	0	-1.972820	0.303808	1.150456
16	1	0	-3.507315	1.082626	0.140474
17	1	0	-1.233828	-0.346454	1.001881

Frequencies -- -564.9137 24.3927 52.1604
Frequencies -- 66.6408 82.8210 107.2179
Frequencies -- 150.2703 180.0324 205.6601
Frequencies -- 250.8057 279.3976 423.9241
Frequencies -- 497.8270 528.0804 559.3172
Frequencies -- 592.0097 699.6568 761.6631
Frequencies -- 837.1282 893.9019 921.6734
Frequencies -- 984.5515 998.2639 1039.8068
Frequencies -- 1048.8616 1070.9004 1080.4061
Frequencies -- 1221.3163 1273.3525 1332.1575
Frequencies -- 1391.6491 1396.0969 1465.5202
Frequencies -- 1477.2916 1530.9983 1735.3118
Frequencies -- 1768.8278 3063.9414 3167.4383
Frequencies -- 3185.2159 3199.8608 3206.8688
Frequencies -- 3257.2876 3297.8634 3725.9709

***syn-trans*-MVK-oxide + FA 1,2-insertion ($TS_{1,2\text{-insertion}}$)**

1	6	0	1.023375	0.095565	0.160477
2	8	0	1.460800	-0.953416	-0.453370
3	8	0	0.895966	-2.167886	0.058231
4	1	0	-0.076820	-1.916625	-0.168482
5	8	0	-1.170538	-0.989519	-0.650328
6	6	0	-2.175145	-0.266088	-0.330666
7	8	0	-2.166801	0.765638	0.355662
8	1	0	-3.141474	-0.613458	-0.739514
9	6	0	0.464545	0.088865	1.519176
10	6	0	1.294135	1.303548	-0.581909
11	6	0	0.639211	2.435838	-0.303241
12	1	0	1.034286	0.796825	2.120203
13	1	0	-0.574925	0.439397	1.441206
14	1	0	0.492967	-0.903919	1.947156

15	1	0	1.945154	1.212014	-1.438960
16	1	0	-0.091443	2.487184	0.489267
17	1	0	0.780111	3.313679	-0.915453

Frequencies --	-163.9269	55.7009	69.5916
Frequencies --	97.8697	155.8109	213.5566
Frequencies --	249.7706	275.2135	294.0929
Frequencies --	338.3040	383.2531	402.5422
Frequencies --	496.7181	579.3271	680.6326
Frequencies --	744.7251	809.4464	913.6348
Frequencies --	947.3907	987.9028	1006.4702
Frequencies --	1036.0714	1055.0691	1074.4474
Frequencies --	1087.8731	1312.4848	1346.3515
Frequencies --	1357.7065	1403.7739	1411.4036
Frequencies --	1433.7237	1474.9757	1492.6662
Frequencies --	1521.2474	1566.6586	1653.9803
Frequencies --	1676.0952	2678.3918	2916.1385
Frequencies --	2933.3398	3099.7182	3183.4906
Frequencies --	3207.7456	3215.8154	3281.6363

MVK-oxide, Dioxole Formation (TS_d)

anti-cis-MVK-oxide = Dioxole

1	6	0	2.113823	0.224472	0.046960
2	6	0	0.631136	0.106616	0.056598
3	6	0	-0.289484	1.134011	0.002167
4	6	0	-1.658696	0.880700	0.034722
5	8	0	0.192038	-1.122782	-0.127554
6	8	0	-1.177527	-1.228705	0.016537
7	1	0	2.550605	-0.538418	-0.594098
8	1	0	2.411928	1.209438	-0.302360
9	1	0	2.509711	0.088426	1.053507
10	1	0	0.081305	2.079491	-0.370189
11	1	0	-2.293385	1.513012	-0.583405
12	1	0	-2.156925	0.385158	0.842006

Frequencies --	-471.2006	129.9630	232.4944
Frequencies --	267.8180	345.0662	520.7306
Frequencies --	585.7959	638.2258	724.1134
Frequencies --	808.1880	912.1419	959.4270
Frequencies --	1042.9633	1044.6798	1056.1667
Frequencies --	1089.9579	1243.2361	1282.7912
Frequencies --	1383.9647	1424.2076	1486.9383
Frequencies --	1498.0863	1540.0503	1595.2316
Frequencies --	3061.7131	3105.9572	3125.9347
Frequencies --	3157.3046	3189.7207	3304.8678

MVK-oxide + HC(O)OH, Dioxole Formation from Spectator Catalysis ($TS_{d,cat}$)

anti-cis-MVK-oxide…FA = Dioxole…FA

1	6	0	-2.135974	-1.600554	-0.223567
2	6	0	-1.469198	-0.276899	-0.123822
3	6	0	-1.453706	0.567260	0.964753
4	6	0	-0.773330	1.778993	0.901700
5	8	0	-0.633003	-0.040766	-1.110808

6	8	0	-0.013864	1.217329	-1.009389
7	1	0	-1.439848	-2.340204	-0.612410
8	1	0	-2.491825	-1.911032	0.754056
9	1	0	-2.989859	-1.540387	-0.898172
10	1	0	-1.663021	0.104698	1.918380
11	1	0	-0.227391	2.093541	1.788265
12	1	0	-1.020845	2.563652	0.214598
13	1	0	1.537967	0.644218	-0.731914
14	8	0	2.453091	0.287033	-0.540926
15	6	0	2.388458	-0.687593	0.352168
16	8	0	1.389434	-1.116902	0.883232
17	1	0	3.392056	-1.075286	0.562921

Frequencies --	-484.5859	31.3998	52.2362
Frequencies --	66.6163	91.4748	132.9860
Frequencies --	196.0533	220.2800	231.1508
Frequencies --	305.9134	351.5718	530.0819
Frequencies --	575.3184	637.7306	694.9380
Frequencies --	709.6615	814.9991	918.8497
Frequencies --	938.8683	1010.9507	1041.3059
Frequencies --	1056.5512	1071.4225	1092.0081
Frequencies --	1098.7011	1229.3687	1246.2301
Frequencies --	1287.7024	1387.9984	1403.2139
Frequencies --	1422.2810	1460.6611	1486.2892
Frequencies --	1492.4166	1544.4523	1603.4700
Frequencies --	1770.9274	3038.8323	3066.8795
Frequencies --	3110.9434	3119.6086	3134.7853
Frequencies --	3169.0056	3206.7122	3289.1762

anti-cis-MVK-oxide…FA = Dioxole…FA Geometry 2

1	6	0	1.854177	1.733388	0.123705
2	6	0	1.279971	0.368525	0.055331
3	6	0	1.456472	-0.568950	-0.939456
4	6	0	0.778288	-1.783990	-0.889753
5	8	0	0.729141	-0.031977	1.185450
6	8	0	0.071347	-1.262297	1.039032
7	1	0	2.191299	1.959422	1.132859
8	1	0	2.679473	1.834122	-0.575483
9	1	0	1.073987	2.442739	-0.150423
10	1	0	2.342483	-0.457100	-1.548247
11	1	0	1.318999	-2.676034	-1.199281
12	1	0	-0.289381	-1.872243	-0.946020
13	1	0	-1.415546	-0.758775	0.597259
14	8	0	-2.337867	-0.505932	0.285841
15	6	0	-2.309546	0.650421	-0.356836
16	8	0	-1.330040	1.324608	-0.584591
17	1	0	-3.318132	0.936287	-0.674475

Frequencies --	-482.6382	48.1541	74.5436
Frequencies --	92.7216	134.4808	151.6611
Frequencies --	206.5350	236.7073	243.7265
Frequencies --	335.4986	347.2842	533.4764
Frequencies --	581.8828	638.0656	703.9008

Frequencies --	716.5556	809.6137	922.2277
Frequencies --	944.2503	1018.4753	1038.8088
Frequencies --	1050.5333	1068.3592	1091.3569
Frequencies --	1113.1034	1229.8195	1237.7700
Frequencies --	1287.1369	1384.3028	1404.2313
Frequencies --	1415.1753	1477.1696	1485.3205
Frequencies --	1498.8356	1550.7078	1607.1082
Frequencies --	1763.6291	2993.5918	3063.4820
Frequencies --	3068.3399	3112.9995	3139.0380
Frequencies --	3163.1134	3201.8645	3277.1725

Products

HPBF Adduct

Optimal Geometry

1	6	0	-0.883500	1.834737	1.149530
2	6	0	-1.034160	0.529419	0.971859
3	1	0	-1.227925	2.310005	2.055163
4	1	0	-0.413804	2.462367	0.407125
5	6	0	-0.655954	-0.226175	-0.267616
6	1	0	-1.504382	-0.086180	1.724944
7	6	0	-1.836046	-0.471726	-1.191482
8	8	0	0.260416	0.584631	-1.104752
9	8	0	-0.134272	-1.492675	-0.000581
10	1	0	-2.188107	0.474285	-1.591477
11	1	0	-1.526585	-1.121755	-2.006710
12	1	0	-2.634634	-0.952142	-0.633379
13	6	0	1.553524	0.719314	-0.833830
14	8	0	0.585099	-1.524915	1.255073
15	8	0	2.195498	0.210024	0.055430
16	1	0	1.998607	1.390186	-1.573964
17	1	0	1.379722	-1.006701	1.006175

Frequencies --	76.0580	98.5864	202.2503
Frequencies --	212.1732	245.6072	272.8544
Frequencies --	294.5828	305.7747	332.8314
Frequencies --	358.7746	474.4106	526.5001
Frequencies --	574.6054	651.3611	692.4755
Frequencies --	702.5520	816.2610	842.2525
Frequencies --	933.1789	971.4580	989.3940
Frequencies --	1026.7452	1051.0041	1054.5359
Frequencies --	1135.5926	1177.0500	1242.5607
Frequencies --	1267.6093	1327.8929	1415.3733
Frequencies --	1422.0245	1461.0687	1496.5053
Frequencies --	1499.6251	1507.1182	1708.6714
Frequencies --	1757.4064	3077.6396	3079.7797
Frequencies --	3160.8343	3172.7541	3174.8347
Frequencies --	3210.0886	3263.1153	3498.3543

syn-trans-HPBF Adduct

1	6	0	0.457237	0.046294	0.005130

2	8	0	-0.075554	1.015498	-0.847125
3	8	0	-1.059222	1.851939	-0.197027
4	8	0	-0.293821	-1.250478	-0.114982
5	6	0	-1.613958	-1.322395	-0.043737
6	8	0	-2.413821	-0.419832	0.077857
7	1	0	-1.917747	-2.370481	-0.116553
8	1	0	-1.801330	1.213890	-0.130503
9	6	0	0.496098	0.423415	1.466002
10	6	0	1.772322	-0.298626	-0.634737
11	6	0	2.945464	-0.315131	-0.017306
12	1	0	0.994455	-0.363908	2.023926
13	1	0	1.034795	1.359260	1.585088
14	1	0	-0.507512	0.555272	1.852386
15	1	0	1.695699	-0.524314	-1.689723
16	1	0	3.051351	-0.090139	1.033042
17	1	0	3.846645	-0.557931	-0.559563

Frequencies --	73.2685	75.1436	188.1957
Frequencies --	237.5739	256.0780	260.8648
Frequencies --	273.0045	302.7491	358.1477
Frequencies --	404.2583	435.7289	498.3230
Frequencies --	570.0881	632.0803	676.6209
Frequencies --	726.4038	813.9231	837.0692
Frequencies --	927.2139	971.4672	978.0580
Frequencies --	1029.4082	1035.4653	1053.2503
Frequencies --	1102.2452	1194.6455	1245.1457
Frequencies --	1317.3552	1340.0749	1418.6744
Frequencies --	1425.7382	1464.0844	1503.3446
Frequencies --	1504.8200	1508.4557	1715.3735
Frequencies --	1742.3090	3079.1638	3091.7916
Frequencies --	3170.2909	3176.0730	3188.2658
Frequencies --	3197.1056	3262.7404	3498.1199

syn-cis-HPBF Adduct

1	6	0	0.432215	-0.145618	0.222804
2	8	0	0.282486	0.928543	-0.646123
3	8	0	-0.616192	1.936191	-0.128090
4	8	0	-0.492551	-1.270172	-0.139827
5	6	0	-1.787431	-1.075427	-0.334991
6	8	0	-2.405668	-0.033666	-0.298601
7	1	0	-2.264329	-2.035409	-0.551756
8	1	0	-1.469893	1.469880	-0.250398
9	6	0	0.222927	0.170168	1.690624
10	6	0	1.782477	-0.748174	-0.050487
11	6	0	2.800194	-0.078783	-0.575293
12	1	0	0.489315	-0.706360	2.275938
13	1	0	0.870494	0.997342	1.967264
14	1	0	-0.805895	0.444888	1.895966
15	1	0	1.877531	-1.784329	0.242571
16	1	0	2.700058	0.953190	-0.873416
17	1	0	3.755828	-0.559354	-0.720982

Frequencies --	73.4005	110.1686	174.4288

Frequencies --	228.9413	254.5921	270.9765
Frequencies --	291.4448	294.5732	352.5409
Frequencies --	383.9210	473.1621	504.2500
Frequencies --	563.3891	653.0899	687.3126
Frequencies --	723.9887	807.4825	833.5515
Frequencies --	930.2589	980.2527	990.3255
Frequencies --	1031.0189	1052.6068	1062.1014
Frequencies --	1102.6922	1204.1195	1252.5150
Frequencies --	1280.7503	1329.9955	1419.0919
Frequencies --	1421.6878	1456.2658	1496.4532
Frequencies --	1500.6437	1502.5567	1707.2892
Frequencies --	1745.0153	3079.6122	3084.1918
Frequencies --	3163.3912	3176.6113	3180.0032
Frequencies --	3202.6234	3271.2006	3509.9004

anti-trans-HPBF Adduct

1	6	0	0.478038	-0.197619	0.338885
2	6	0	1.474202	-0.948701	1.193335
3	6	0	0.990416	0.370788	-0.951236
4	6	0	2.257079	0.313244	-1.342234
5	8	0	-0.100731	0.733612	1.201497
6	8	0	-0.654464	1.875760	0.507737
7	1	0	2.291019	-0.288781	1.468341
8	1	0	1.854392	-1.812727	0.657381
9	1	0	0.972227	-1.283022	2.097192
10	1	0	0.248828	0.840354	-1.577807
11	1	0	3.032076	-0.138917	-0.742348
12	1	0	2.556104	0.733849	-2.290482
13	1	0	-1.450259	1.461522	0.112903
14	8	0	-2.252965	0.072138	-0.627810
15	6	0	-1.723768	-1.008117	-0.478493
16	8	0	-0.508013	-1.274192	-0.028153
17	1	0	-2.230804	-1.948393	-0.712893

Frequencies --	67.2305	78.6126	190.4383
Frequencies --	230.7580	261.1112	271.1780
Frequencies --	295.9908	316.7984	332.7954
Frequencies --	386.2570	431.9330	497.3510
Frequencies --	555.9419	640.5126	674.8534
Frequencies --	747.3335	796.6004	827.2875
Frequencies --	929.1544	981.2899	987.2412
Frequencies --	1030.0845	1039.4254	1053.3609
Frequencies --	1098.2499	1196.5287	1249.4094
Frequencies --	1319.5076	1347.4390	1417.2472
Frequencies --	1423.6114	1465.4914	1500.4579
Frequencies --	1503.5173	1509.4884	1708.8719
Frequencies --	1742.8042	3078.8912	3086.7923
Frequencies --	3167.6353	3176.1550	3178.7332
Frequencies --	3226.9347	3262.8343	3513.2659

anti-cis-HPBF Adduct

1	6	0	0.442256	0.538765	-0.117107

2	6	0	1.238904	1.769289	-0.517064
3	6	0	1.028468	-0.153815	1.079460
4	6	0	1.865296	-1.181875	1.034309
5	8	0	0.316607	-0.189194	-1.293323
6	8	0	-0.021159	-1.585110	-1.103847
7	1	0	2.245016	1.464290	-0.787545
8	1	0	1.280360	2.465937	0.315370
9	1	0	0.758387	2.250474	-1.365607
10	1	0	0.777690	0.314395	2.021856
11	1	0	2.120935	-1.666049	0.105950
12	1	0	2.299573	-1.569839	1.943632
13	1	0	-0.895132	-1.503203	-0.664768
14	8	0	-2.122731	-0.762499	0.291004
15	6	0	-1.957663	0.418659	0.502294
16	8	0	-0.865209	1.141113	0.312152
17	1	0	-2.750456	1.063374	0.891870

Frequencies -- 54.9770 93.2607 192.8808
Frequencies -- 219.1618 241.6570 261.2429
Frequencies -- 293.4247 303.6928 333.2523
Frequencies -- 345.9031 457.1580 495.2571
Frequencies -- 557.1344 649.6134 680.8966
Frequencies -- 720.5570 795.0306 828.8901
Frequencies -- 928.0345 982.6728 993.0687
Frequencies -- 1026.6763 1054.9804 1063.3948
Frequencies -- 1100.0391 1183.3306 1244.3178
Frequencies -- 1292.9461 1334.9574 1413.7217
Frequencies -- 1418.8021 1461.7654 1496.2762
Frequencies -- 1498.5126 1528.3769 1706.7824
Frequencies -- 1749.0678 3078.7048 3080.2442
Frequencies -- 3162.2933 3174.6873 3176.8041
Frequencies -- 3192.5660 3276.2360 3478.1191

2-alkoxy-but-3-en-2-yl formate (**ABF)**

1	6	0	2.372674	-1.020834	-0.081462
2	6	0	1.802909	0.171921	0.034423
3	1	0	3.448819	-1.110346	-0.098440
4	1	0	1.785744	-1.919485	-0.181417
5	6	0	0.297368	0.406274	0.068797
6	1	0	2.382535	1.074785	0.156943
7	6	0	-0.114558	1.570558	-0.832022
8	8	0	0.074864	0.636804	1.370559
9	8	0	-0.331173	-0.831697	-0.394272
10	1	0	0.095177	1.310963	-1.866845
11	1	0	0.457472	2.451934	-0.554932
12	1	0	-1.172513	1.773592	-0.706715
13	6	0	-1.655823	-0.957260	-0.204460
14	8	0	-2.399740	-0.137245	0.260446
15	1	0	-1.964267	-1.948301	-0.554118

Frequencies -- 62.0861 107.9899 173.0780
Frequencies -- 223.5841 239.7966 262.0089
Frequencies -- 307.7685 348.7095 425.4105

Frequencies --	511.1594	545.8325	649.3337
Frequencies --	691.0476	828.4077	891.6562
Frequencies --	951.9134	987.3386	1018.9171
Frequencies --	1034.7477	1043.9681	1102.8519
Frequencies --	1162.2461	1169.2324	1230.4460
Frequencies --	1324.1390	1399.1923	1412.1628
Frequencies --	1443.1028	1491.2506	1513.5205
Frequencies --	1685.8150	1784.4604	3057.9617
Frequencies --	3078.6667	3160.3187	3178.1332
Frequencies --	3184.1275	3215.5311	3276.1918

HPBD

syn-trans-HPBD

1	6	0	-2.464345	-0.116911	0.238336
2	6	0	-1.300331	-0.569685	-0.223392
3	6	0	-0.023440	0.144293	-0.096181
4	6	0	0.153909	1.464923	-0.121176
5	8	0	0.974393	-0.800835	0.028511
6	8	0	2.277865	-0.181514	0.024577
7	1	0	2.519831	-0.297426	0.953085
8	1	0	-2.533913	0.816122	0.778558
9	1	0	-3.375915	-0.673859	0.083750
10	1	0	-1.248384	-1.528655	-0.722786
11	1	0	-0.703042	2.098371	-0.274497
12	1	0	1.128601	1.908518	-0.028332

Frequencies --	91.1217	140.1924	169.7015
Frequencies --	243.2428	349.8817	408.7866
Frequencies --	502.1832	589.5903	736.3323
Frequencies --	745.8301	849.6965	868.4701
Frequencies --	922.0106	964.0224	976.9689
Frequencies --	1028.0828	1089.9308	1240.0390
Frequencies --	1331.5374	1387.2291	1427.9310
Frequencies --	1469.2457	1693.9399	1701.3359
Frequencies --	3168.0011	3184.9250	3209.6562
Frequencies --	3259.4138	3308.4327	3771.5467

syn-cis-HPBD

1	6	0	-2.190756	-0.692912	-0.003071
2	6	0	-1.445754	0.413306	0.020214
3	6	0	0.013806	0.455029	-0.002236
4	6	0	0.721715	1.588008	-0.003222
5	8	0	0.539944	-0.815903	-0.022748
6	8	0	1.979630	-0.777544	-0.088691
7	1	0	2.195300	-1.033111	0.818326
8	1	0	-1.747752	-1.675824	-0.043861
9	1	0	-3.267941	-0.629017	0.014193
10	1	0	-1.915634	1.386564	0.056377
11	1	0	0.189628	2.524463	0.015143
12	1	0	1.795734	1.593910	-0.038780

Frequencies --	99.0342	162.6828	176.4313
Frequencies --	230.8765	363.0424	454.0321

Frequencies --	488.9352	579.9838	730.7037
Frequencies --	765.9635	852.2737	856.3530
Frequencies --	927.7028	954.1402	983.4222
Frequencies --	1022.9381	1069.6216	1323.0288
Frequencies --	1327.5623	1390.0403	1423.6910
Frequencies --	1468.7354	1652.4983	1716.5707
Frequencies --	3177.2189	3195.4080	3207.3442
Frequencies --	3269.2861	3308.8785	3767.8216

anti-trans-HPBD

1	6	0	2.069742	-0.797939	-0.201142
2	6	0	0.879834	-0.636682	0.374692
3	6	0	-0.000569	0.507687	0.128656
4	6	0	0.381169	1.765231	-0.109365
5	8	0	-1.353529	0.296846	0.281053
6	8	0	-1.705151	-0.935857	-0.435125
7	1	0	-2.223304	-1.369313	0.254952
8	1	0	2.434117	-0.099974	-0.941304
9	1	0	2.701239	-1.637326	0.047202
10	1	0	0.509155	-1.377298	1.071012
11	1	0	1.420127	2.040287	-0.035189
12	1	0	-0.352948	2.525925	-0.321141

Frequencies --	113.0745	121.3547	200.1393
Frequencies --	249.5238	303.3254	430.7176
Frequencies --	516.4303	557.4750	739.1487
Frequencies --	753.9756	828.3306	876.4466
Frequencies --	900.0855	962.3258	975.0875
Frequencies --	1020.7666	1090.5332	1245.4733
Frequencies --	1333.1117	1379.4282	1420.9404
Frequencies --	1468.9497	1683.9993	1691.8021
Frequencies --	3166.6610	3186.0957	3190.9837
Frequencies --	3258.0684	3289.4386	3786.3994

anti-cis-HPBD

1	6	0	2.006728	-0.206092	0.130891
2	6	0	0.923509	-0.922618	-0.169353
3	6	0	-0.450908	-0.491134	0.058825
4	6	0	-1.523980	-1.275577	-0.081242
5	8	0	-0.667196	0.774334	0.577688
6	8	0	-0.175382	1.761679	-0.392059
7	1	0	-1.017223	2.018838	-0.790669
8	1	0	1.927156	0.783354	0.553037
9	1	0	2.995465	-0.600597	-0.047377
10	1	0	1.027080	-1.910009	-0.600254
11	1	0	-1.411493	-2.313506	-0.353075
12	1	0	-2.512460	-0.893666	0.118584

Frequencies --	115.5187	151.2819	207.7804
Frequencies --	233.2235	317.4068	424.1100
Frequencies --	487.0421	610.5668	738.5384
Frequencies --	765.7953	838.3784	864.7669
Frequencies --	913.2348	962.9370	971.9975

Frequencies --	1024.6076	1062.1145	1312.5338
Frequencies --	1326.5261	1362.7279	1412.5634
Frequencies --	1469.7362	1649.4072	1711.9771
Frequencies --	3174.9533	3182.5028	3187.7437
Frequencies --	3272.1195	3279.5509	3769.7587

HPBD-2

cis-HPBD-2

1	6	0	2.317255	-0.082131	-0.008589
2	6	0	1.034673	0.155715	0.013236
3	6	0	-0.237919	0.453645	0.003115
4	6	0	-0.818488	1.832443	-0.002134
5	8	0	-1.267177	-0.475261	0.018225
6	8	0	-0.746161	-1.811628	-0.116279
7	1	0	2.892995	-0.185416	0.903526
8	1	0	2.857427	-0.191956	-0.941420
9	1	0	-0.020776	2.568205	0.012381
10	1	0	-1.426278	1.979665	-0.894237
11	1	0	-1.455743	1.981111	0.869162
12	1	0	-0.514049	-2.014530	0.801259

Frequencies --	123.2222	147.2663	159.6806
Frequencies --	181.9859	234.3641	289.3167
Frequencies --	436.0598	472.8574	643.6710
Frequencies --	650.5356	775.7473	923.3288
Frequencies --	930.8642	1007.2837	1039.6457
Frequencies --	1073.8875	1198.1988	1337.1285
Frequencies --	1398.8254	1417.6773	1486.2407
Frequencies --	1492.7342	1523.0317	2064.9205
Frequencies --	3058.6458	3119.5494	3122.8748
Frequencies --	3165.8351	3193.5637	3743.3575

trans-HPBD-2

1	6	0	2.520720	-0.452916	-0.134163
2	6	0	1.280534	-0.073369	-0.011105
3	6	0	0.030621	0.291993	0.127942
4	6	0	-0.518009	1.665903	-0.079347
5	8	0	-0.848147	-0.667322	0.619027
6	8	0	-1.947144	-0.805672	-0.349262
7	1	0	3.202389	-0.446108	0.706916
8	1	0	2.914244	-0.784465	-1.086628
9	1	0	0.266176	2.344762	-0.402154
10	1	0	-1.303059	1.644464	-0.832389
11	1	0	-0.953598	2.034525	0.849242
12	1	0	-1.647028	-1.598896	-0.813060

Frequencies --	81.9338	167.1076	178.1649
Frequencies --	237.5646	255.7472	321.4638
Frequencies --	421.5491	523.2995	588.0691
Frequencies --	667.1507	784.2386	839.3043
Frequencies --	913.4833	994.7043	1028.8299
Frequencies --	1073.8319	1193.2906	1308.4319
Frequencies --	1346.2114	1415.4147	1482.7656

Frequencies --	1487.5845	1514.2043	2052.0952
Frequencies --	3061.3715	3128.6071	3136.2007
Frequencies --	3157.8898	3210.5376	3765.1591

SOZ

1	6	0	0.605263	0.119462	0.017252
2	8	0	0.045851	-0.112114	1.323349
3	8	0	-1.358215	0.169470	1.094850
4	6	0	-1.588881	-0.553473	-0.111683
5	8	0	-0.410389	-0.370511	-0.866370
6	8	0	-2.698050	-0.058363	-0.729262
7	1	0	-1.762655	-1.608381	0.091917
8	1	0	-2.508660	0.851960	-0.987028
9	6	0	0.836912	1.594589	-0.227548
10	6	0	1.804261	-0.773946	-0.074132
11	6	0	3.050189	-0.370618	-0.289551
12	1	0	1.612216	1.974167	0.433045
13	1	0	1.126337	1.762698	-1.262014
14	1	0	-0.084833	2.132415	-0.024024
15	1	0	1.573543	-1.823569	0.047834
16	1	0	3.305308	0.670396	-0.418315
17	1	0	3.858708	-1.083618	-0.347974

Frequencies --	67.8607	73.2070	205.2698
Frequencies --	247.6267	277.8925	305.3963
Frequencies --	322.7793	392.1122	414.9188
Frequencies --	474.5515	487.6597	572.6376
Frequencies --	656.9024	679.2307	724.7180
Frequencies --	818.0148	901.2113	920.3294
Frequencies --	941.6198	983.1285	990.4383
Frequencies --	1018.8756	1029.1674	1046.6565
Frequencies --	1144.5795	1177.9216	1211.4823
Frequencies --	1298.5922	1331.6679	1342.3299
Frequencies --	1345.8385	1416.4678	1454.8866
Frequencies --	1463.6620	1502.1686	1511.7156
Frequencies --	1710.9530	3076.4739	3112.6541
Frequencies --	3157.3922	3160.9413	3175.0021
Frequencies --	3196.3289	3261.8504	3797.2718

Geometry 2

1	6	0	0.583489	0.195188	-0.044411
2	8	0	-0.153576	0.277939	1.181437
3	8	0	-1.407243	0.864245	0.707581
4	6	0	-1.675214	0.053805	-0.422636
5	8	0	-0.414305	-0.211552	-0.990523
6	8	0	-2.369317	-1.097403	-0.135870
7	1	0	-2.294460	0.646443	-1.089925
8	1	0	-1.830842	-1.626561	0.463977
9	6	0	1.163029	1.535949	-0.438873
10	6	0	1.556535	-0.929945	0.141014
11	6	0	2.876527	-0.825241	0.055522

12	1	0	1.907361	1.857085	0.285356
13	1	0	1.618195	1.469085	-1.423784
14	1	0	0.363402	2.270026	-0.467536
15	1	0	1.089967	-1.882977	0.351124
16	1	0	3.367273	0.111544	-0.160607
17	1	0	3.508436	-1.689028	0.196713

Frequencies -- 69.4712 74.8706 184.3687
Frequencies -- 256.1995 291.1910 298.8414
Frequencies -- 306.9989 359.2658 425.2914
Frequencies -- 485.8813 539.9597 575.0712
Frequencies -- 663.7208 674.9655 800.0369
Frequencies -- 817.4105 867.3488 901.4383
Frequencies -- 939.2299 966.2538 984.4719
Frequencies -- 1002.5508 1024.2063 1046.1675
Frequencies -- 1124.0878 1146.8876 1203.9039
Frequencies -- 1294.6568 1312.1961 1321.7208
Frequencies -- 1335.5380 1417.7963 1446.8489
Frequencies -- 1462.5576 1502.5040 1510.9146
Frequencies -- 1711.3281 3078.9022 3147.4541
Frequencies -- 3158.3426 3167.3113 3175.5891
Frequencies -- 3193.3870 3263.3750 3805.5868

Dioxole

1	6	0	-2.167553	0.060489	-0.004807
2	6	0	-0.683232	0.125915	-0.003925
3	6	0	0.170081	1.143757	-0.033828
4	6	0	1.554460	0.584898	0.051521
5	8	0	-0.085539	-1.098560	0.054088
6	8	0	1.362919	-0.838086	-0.081663
7	1	0	-2.525051	-0.449745	0.888636
8	1	0	-2.582146	1.063800	-0.028217
9	1	0	-2.524516	-0.494143	-0.871307
10	1	0	-0.084916	2.186780	-0.064608
11	1	0	2.044633	0.802223	1.007160
12	1	0	2.210411	0.893894	-0.764831

Frequencies -- 91.1365 158.0101 224.3964
Frequencies -- 328.3782 558.4446 624.7729
Frequencies -- 710.0235 755.0948 830.1219
Frequencies -- 928.9588 970.0706 1025.9198
Frequencies -- 1037.0761 1058.7527 1078.5195
Frequencies -- 1184.0051 1220.5280 1299.6887
Frequencies -- 1371.3908 1425.1484 1486.1439
Frequencies -- 1503.4467 1539.6591 1739.4168
Frequencies -- 2995.1827 3056.1346 3064.3626
Frequencies -- 3125.3228 3161.7358 3281.3841

OBD...FA + OH

1	6	0	-2.229908	2.605921	0.000000
2	6	0	-2.340609	1.278466	0.000000
3	6	0	-1.144980	0.401021	0.000000
4	6	0	-1.353939	-1.017300	0.000000

5	8	0	-0.000000	0.884653	0.000000
6	1	0	-1.252242	3.066174	0.000000
7	1	0	-3.098903	3.246071	0.000000
8	1	0	-3.309606	0.798664	0.000000
9	1	0	-2.354062	-1.422347	0.000000
10	1	0	-0.496548	-1.674922	0.000000
11	8	0	2.462717	-0.194105	0.000000
12	6	0	2.539514	-1.514397	0.000000
13	1	0	1.515209	0.101318	0.000000
14	1	0	3.586529	-1.835444	0.000000
15	8	0	1.610927	-2.290771	0.000000

Frequencies --	36.9248	49.9848	104.7519
Frequencies --	113.3620	131.9970	178.3828
Frequencies --	204.9212	314.8904	402.4129
Frequencies --	448.2982	485.4281	619.8588
Frequencies --	690.6406	727.3866	820.7788
Frequencies --	872.4641	953.1017	1014.5611
Frequencies --	1016.4360	1026.9626	1083.9120
Frequencies --	1100.0746	1224.3791	1272.9143
Frequencies --	1344.1951	1400.9060	1444.6482
Frequencies --	1455.3042	1499.7777	1615.3304
Frequencies --	1682.0530	1774.7684	3059.8447
Frequencies --	3156.9986	3170.9939	3196.7681
Frequencies --	3268.3070	3271.3896	3288.7752

References

1. C. Huang, B. Yang and F. Zhang, J. Chem. Phys. **150**, 164305 (2019).
2. R. L. Caravan, M. F. Vansco, K. Au, M. A. H. Khan, Y.-L. Li, F. A. F. Winiberg, K. Zuraski, Y.-H. Lin, W. Chao, N. Trongsiriwat, P. J. Walsh, D. L. Osborn, C. J. Percival, J. J.-M. Lin, D. E. Shallcross, L. Sheps, S. J. Klippenstein, C. A. Taatjes and M. I. Lester, Proc. Natl. Acad. Sci. **117**, 9733-9740 (2020).
3. M. Kumar, D. H. Busch, B. Subramaniam and W. H. Thompson, Phys. Chem. Chem. Phys. **16** (42), 22968-22973 (2014).
4. L. Vereecken, Phys. Chem. Chem. Phys. **19**, 28630-28640 (2017).
5. V. P. Barber, S. Pandit, A. M. Green, N. Trongsiriwat, P. J. Walsh, S. J. Klippenstein and M. I. Lester, J. Am. Chem. Soc. **140**, 10866-10880 (2018).
6. T. A. Burd, X. Shan and D. C. Clary, Phys. Chem. Chem. Phys. **20**, 25224-25234 (2018).
7. A. W. Jasper, Internation Journal of Chemical Kinetics **52**, 387-402 (2020).
8. J. K. Klassen and G. M. Nathanson, **273**, 333-335 (1996).
9. S. Miura, M. E. Tuckerman and M. L. Klein, J. Chem. Phys. **109**, 5290-5299 (1998).
10. D. Luckhaus, Phys. Chem. Chem. Phys. **12**, 8357-8361 (2010).
11. Y.-S. Wang, K.-L. Shen and S. D. Chao, ChJPh **55**, 719-728 (2017).
12. T. Järvinen, J. Lundell and P. Dopieralski, Theor. Chem. Acc. **137**, 1-8 (2018).
13. S. Gómez, Y. Oueis, A. Restrepo and A. Wasserman, Int. J. Quantum. Chem. **119**, 1-9 (2019).
14. N. J. Leonard, J. Am. Chem. Soc. **79**, 6210-6214 (1957).